Electronic Supplementary Material (ESI) for Journal of Materials Chemistry C
This journal is © The Royal Society of Chemistry 2021

Electronic Supplementary Information for

Facile ACQ-to-AIE transformation *via* diphenylphosphine (DPP) modification with versatile properties

Fangjun Ye,[a] Chengzhen Shen,[a] Jianxin Guan,[a] Yiming Liu,[a] Xiaoge Wang,[a] Jingtian Wang,[b] Ming Cong,[b] Weibin Wang,[b] Ting Zhang,[b] Bo Zou,*[b] Junrong Zheng,*[a] Yuguo Ma*[a]

a. *College of Chemistry and Molecular Engineering, Beijing National Laboratory for Molecular Sciences, Peking University, Beijing 100871, China*
b. *State Key Laboratory of Superhard Materials, College of Physics, Jilin University, Changchun 130012, China*

Table of Contents

1. Experimental Procedures

1.1 Material and Methods

Materials: All the reactions sensitive to oxygen were performed under N_2 through standard Schlenk technique. All the reactions sensitive to moisture were performed using the drying tube equipped with $CaCl_2$. All reagents were purchased from commercial suppliers and used directly unless otherwise specified. CH_2Cl_2 (DCM) and Et_3N were distilled under N_2 atmosphere with CaH_2, and toluene were distilled under N_2 atmosphere with sodium. The crystallizations from dichloromethane and petroleum ether afford single crystals suitable for structure determination.

Instruments: NMR spectra were recorded on a Bruker Advance 400 MHz spectrometer, using $CDCl_3$, DMSO-d_6 or D_6-acetone as solvent. Chemical shifts are reported as part per million (ppm) relative to the internal referenced TMS. High resolution mass spectra (HR-MS) were recorded on a Bruker Apex IV FTMS mass spectrometers, using electrospray ionization (ESI) mode. UV-Vis absorption spectra were measured by using Hitachi U-4100 spectrophotometer. The photometer is equipped with a R928 photomultiplier tube (180-850 nm) and excitation light source is a 150 W xenon lamp where the excitation light path is perpendicular to the detection light path. Absolute photoluminescence quantum yield, transient fluorescence decay characteristics and temperature-dependent photoluminescence spectra were measured on Edinburgh Instrument FLS980 spectrometer equipped with an integrating sphere (N-M01), a picosecond pulsed diode laser (EPL-365) and a closed cycle cryostate respectively. XRD data were collected on powder X-ray diffractometer (X-Pert3 Powder) and single crystal X-ray diffractometer (XtaLAB PRO 007HF(Mo)) respectively. High pressure experiments were performed using symmetric diamond anvil cells (DACs) at room temperature. The culet diameter of the diamond anvils was 500 μm. The sample was placed in the holes (diameter: ca. 170 μm) of a T301 steel gasket, which was pre-indented to a thickness of 50 μm. The silicon oil was used as pressure transmitting medium (PTM) in high-pressure photoluminescence and UV-Vis absorption experiments. A small ruby chip was inserted into the sample compartment for in-situ pressure calibration according to the R1 ruby fluorescence method. The 405 nm line of a laser with a power of 100 mW was used for pressure calibration. The photoluminescence measurements under high pressure were performed on a QE65000 Scientific-grade spectrometer in the reflection mode. The 355 nm line of a laser with a power of 10 mW was used as the excitation source. The in-situ UV/Vis absorption measurements under high pressure were performed on an Ocean Optics QE65000 Scientific-grade spectrometer. In situ PL and absorption photographs were recorded by camera (Canon Eos 5D mark Ⅱ) equipped on a microscope (Ecilipse TI-U, Nikon). The ultrafast measurements were performed with laser pulses (1 kHz, ~50 fs pulse width, 800 nm central wavelength) from an amplified Ti/sapphire laser system (Uptek Solutions Inc.).

Calculation methods: To confirm the mechanism, calculations on the structures were carried out. The M06-2X[1] is used in combination with 6-31g** basis set to compute the equilibrium structures and vibrational frequencies.[2] These calculations were performed with the Gaussian 09 software.[3] The SOC constant was computed by orca.[4]

1.2 Synthesis and Characterization

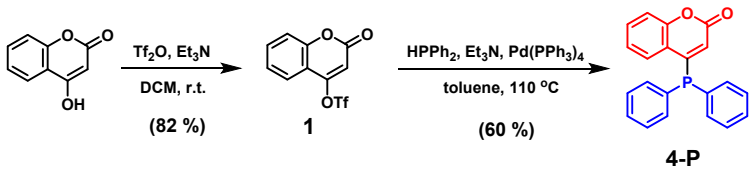

Compound 1 was synthesized according to the literature procedure[5]. A dry round-bottom flask, equipped with a magnetic stirring bar and a septum, was charged with 1 g of 4-hydroxycoumarin (6.2 mmol, 1.0 equiv), NEt_3 (1.12 mL, 1.3 equiv) and CH_2Cl_2 (25 mL). The mixture was cooled to 0 °C and trifluoromethanesulfonic anhydride (8 mmol, 1.3 equiv) was added dropwise. The reaction was then warm to room temperature and stirred for overnight. Then the solvents were evaporated under reduced pressure and the residue was subjected to column chromatography purification on silica, yielding the respective triflate **1** (1.5 g, 82%).

^{1}H NMR (400 MHz, DMSO-d_6) δ 7.82 (ddd, J = 8.7, 7.3, 1.6 Hz, 1H), 7.77-7.66 (m, 1H), 7.59 (dd, J = 8.4, 1.1 Hz, 1H), 7.56-7.51 (m, 1H), 6.91 (s, 1H).

4-P: A dry and nitrogen flushed Schlenk tube, equipped with a magnetic stirring bar, was charged with 200 mg **1** (0.7 mmol, 1 equiv) and 12 mg $Pd(PPh_3)_4$ (0.01 mmol, 0.015 equiv), and dissolved in NEt_3 (0.28 mL, 3 equiv), $HPPh_2$ (0.13 mL, 1.1 equiv) and toluene (5 mL). The mixture was heated to 110 °C and stirred for overnight. The reaction progress was monitored by thin-layer chromatography (TLC). Upon completion the solvents were evaporated and the residue was subjected to column chromatography purification on silica yielding the respective product **4-P** (134 mg, 60%).

^{1}H NMR (400 MHz, Chloroform-d) δ 7.72 (ddd, J = 8.0, 3.0, 1.6 Hz, 1H), 7.55-7.30 (m, 12H), 7.12 (ddd, J = 8.3, 7.3, 1.3 Hz, 1H), 5.92 (d, J = 3.5 Hz, 1H); ^{13}C NMR (100 MHz, $CDCl_3$) δ 159.6, 159.6, 156.9, 156.6, 152.8, 152.8, 134.7, 134.5, 132.1, 132.0, 131.7, 130.2, 129.3, 129.2, 127.0, 126.8, 124.1, 124.1, 120.7, 120.7, 120.2, 120.0, 117.1, 117.1; ^{31}P NMR (200 MHz, $CDCl_3$) δ -14.0; HR-MS (ESI): m/z cal for $C_{21}H_{16}O_2P$ $[M+H]^+$: 331.0882; found: 331.0887.

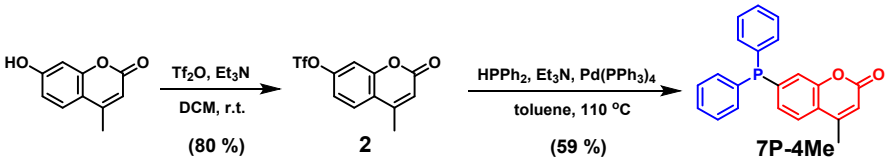

Compound 2 was synthesized according to the literature procedure[5]. A dry round-bottom flask, equipped with a magnetic stirring bar and a septum, was charged with 1 g of 4-hydroxycoumarin (5.7 mmol, 1.0 equiv) dissolved in NEt_3 (1.02 mL, 1.3 equiv) and CH_2Cl_2 (25 mL). The mixture was cooled to 0 °C and trifluoromethanesulfonic anhydride (7.4 mmol, 1.3 equiv) was added dropwise. The reaction was allowed to warm to room temperature and stirred for overnight. Then the solvents were evaporated and the residue was subjected to column chromatography purification on silica yielding the respective triflate **2**. (1.4 g, 80%)
^{1}H NMR (400 MHz, Chloroform-*d*) δ 7.71 (d, J = 8.7 Hz, 1H), 7.40-7.17 (m, 2H), 6.36 (d, J = 1.5 Hz, 1H), 2.47 (d, J = 1.3 Hz, 3H).

7P-4Me: Following a similar procedure for **4-P**, a dry and nitrogen flushed Schlenk tube, equipped with a magnetic stirring bar, was charged with 500 mg **2** (1.6 mmol, 1 equiv) and 28 mg $Pd(PPh_3)_4$ (0.02 mmol, 0.015 equiv) dissolved in NEt_3 (0.68 mL, 3 equiv), $HPPh_2$ (0.28 mL, 1.1 equiv) and toluene (5 mL). The mixture was heated to 110 °C and stirred for overnight. The reaction progress was monitored by TLC (1:4 ethyl acetate (EA)/petroleum ether). Upon completion the solvents were evaporated and the residue was subjected to column chromatography purification on silica yielding the respective product **7P-4Me** (491 mg, 88%).
^{1}H NMR (400 MHz, Chloroform-*d*) δ 7.54 (dd, *J* = 8.1, 1.7 Hz, 1H), 7.44-7.23 (m, 11H), 7.11 (dd, *J* = 6.0, 1.4 Hz, 1H), 6.28 (d, *J* = 1.4 Hz, 1H), 2.42 (d, *J* = 1.2 Hz, 3H); ^{13}C NMR (100 MHz, $CDCl_3$) δ 160.5, 153.4, 153.3, 152.1, 143.9, 143.7, 135.7, 135.6, 134.1, 133.9, 129.4, 129.0, 128.9, 128.8, 124.3, 124.2, 121.3, 121.1, 119.8, 115.4, 18.6; ^{31}P NMR (200 MHz, $CDCl_3$) δ -4.8; HR-MS (ESI): m/z cal for $C_{22}H_{18}O_2P$ $[M+H]^+$: 345.1039; found: 345.1043.

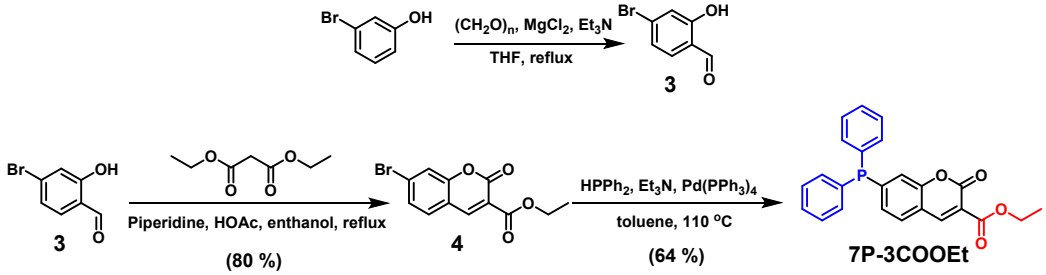

Compound 3: Following a modified procedure from literature[6], to a dry round-bottom flask containing a solution of 10.6 mL Et_3N (80 mmol, 4 equiv) and 4.2 g paraformaldehyde (138 mmol, 7 equiv) in THF (100 mL) was added 3.46 g 3-bromophenol (20 mmol, 1 equiv) and 2.86 g $MgCl_2$ (30 mmol, 1.5 equiv). The mixture was stirred intensely below 45 °C, then was heated to reflux at 80 °C for overnight. The reaction was deemed completed by TLC (1:2 DCM/petroleum ether) with complete consumption of starting material. The reaction mixture was cooled to room temperature, adjusted to pH 1 with 1 M aqueous HCl, and then extracted with EA. The combined organic layers were washed with water, brine, dried over anhydrous Na_2SO_4, filtered and concentrated under vacuum to give crude 4-bromo-2-hydroxybenzaldehyde **3** (4 g, 99%) as yellow oil. This compound was used directly without further purification.
^{1}H NMR (400 MHz, Chloroform-*d*) δ 11.12 (d, J = 1.3 Hz, 1H), 9.89-9.78 (m, 1H), 7.41 (dd, J = 8.2, 1.9 Hz, 1H), 7.23-7.13 (m, 2H).

Compound **4**: Following a modified procedure from literature[7], a dry round-bottom flask equipped with a magnetic stirring bar, was charged with 2 g of compound **3** (10 mmol, 1 equiv), 3.2 g diethylmalonate (20 mmol, 2 equiv), 80 mg piperidine (0.1 mmol, 0.1 equiv) and 60 mg HOAc (0.1 mmol, 0.1 equiv) in 50 mL ethanol. The mixture was heated to reflux for 4 h. The reaction was deemed completed by TLC (1:5 EA/petroleum ether) with complete consumption of starting material. The reaction mixture was cooled to room temperature. The portion of solvents were evaporated and water was added to the mixture to obtain product as a crystalline solid (2.4 g, 80%).
1H NMR (400 MHz, Chloroform-*d*) δ 8.49 (d, J = 0.7 Hz, 1H), 7.55 (d, J = 1.0 Hz, 1H), 7.47 (d, J = 1.1 Hz, 2H), 4.42 (q, J = 7.1 Hz, 2H), 1.41 (t, J = 7.1 Hz, 3H).

7P-3COOEt: Following a similar procedure for **4-P**, a dry and nitrogen flushed Schlenk tube equipped with a magnetic stirring bar was charged with 500 mg **4** (1.7 mmol, 1 equiv) and 29 mg $Pd(PPh_3)_4$ (0.03 mmol, 0.015 equiv), dissolved in NEt_3 (0.7 mL, 3 equiv), $HPPh_2$ (0.29 mL, 1.1 equiv) and toluene (5 mL). The mixture was heated to 110 °C and stirred for overnight. The reaction progress was monitored by TLC (1:2 EA/petroleum ether). Then the solvents were evaporated and the residue was subjected to column chromatography purification on silica yielding the respective product **7P-3COOEt** (420 mg, 64%).
^{1}H NMR (400 MHz, Chloroform-*d*) δ 8.50 (s, 1H), 7.53 (dd, J = 7.9, 1.8 Hz, 1H), 7.45-7.27 (m, 11H), 7.10-7.06 (m, 1H), 4.41 (q, J = 7.1 Hz, 2H), 1.40 (t, J = 7.1 Hz, 3H); ^{13}C NMR (100 MHz, $CDCl_3$) δ 163.0, 156.6, 154.9, 154.8, 148.3, 148.2, 148.0, 135.0, 134.9, 134.3, 134.1, 129.7, 129.3, 129.04, 129.00, 128.9, 128.85, 128.77, 120.5, 120.4, 118.2, 117.5, 62.0, 14.3; ^{31}P NMR (200 MHz, $CDCl_3$) δ -3.0; HR-MS (ESI): m/z cal for $C_{24}H_{20}O_4P$ $[M+H]^+$: 403.1094; found: 403.1096.

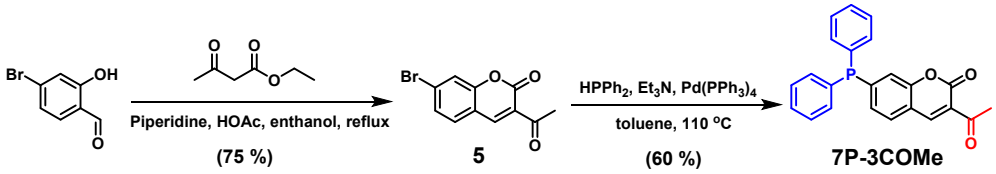

Compound 5: Following a modified procedure for compound **4**, a dry round-bottom flask equipped with a magnetic stirring bar was charged with 0.2 g compound **3** (1 mmol, 1 equiv), 0.26 g diethylmalonate (2 mmol, 2 equiv), 0.8 mg piperidine (0.01 mmol, 0.1 equiv) in 10 mL ethanol. The mixture was heated to reflux for 4 h. The reaction mixture was deemed complete by TLC (1:5 EA/petroleum ether) with complete consumption of starting material. The reaction mixture was cooled to room temperature to obtain product as a crystalline solid (200 mg, 75%).
^{1}H NMR (400 MHz, Chloroform-*d*) δ 8.47 (s, 1H), 7.57 (d, J = 1.6 Hz, 1H), 7.54-7.40 (m, 2H), 2.72 (s, 3H).

7P-3COMe: Following a similar procedure for **4-P**, a dry and nitrogen flushed Schlenk tube equipped with a magnetic stirring bar was charged with 100 mg **5** (0.37 mmol, 1 equiv) and 7 mg $Pd(PPh_3)_4$ (0.006 mmol, 0.015 equiv), dissolved in NEt_3 (0.14 mL, 3 equiv), $HPPh_2$ (0.06 mL, 1.1 equiv) and toluene (2 mL). The mixture was heated to 110 °C and stirred for overnight. The reaction progress was monitored by TLC (1:2 EA/petroleum ether). Then the solvents were evaporated and the residue was subjected to column chromatography purification on silica to yield the respective product **7P-3COMe** (83 mg, 60%).
^{1}H NMR (400 MHz, Chloroform-*d*) δ 8.48 (s, 1H), 7.57 (d, J = 7.9, 1H), 7.45-7.28 (m, 11H), 7.11 (d, J = 7.9, 1H), 2.71 (s, 3H); ^{13}C NMR (100 MHz, $CDCl_3$) δ 195.3, 159.1, 155.0, 154.9, 148.4, 148.2, 147.1, 135.0, 134.9, 134.3, 134.1, 129.7, 129.6, 129.5, 129.4, 129.2, 129.0, 128.9, 124.4, 120.4, 120.2, 117.8, 30.6; ^{31}P NMR (200 MHz, $CDCl_3$) δ -2.8; HR-MS (ESI): m/z cal for $C_{23}H_{18}O_3P$ $[M+H]^+$: 373.0988; found: 373.0982.

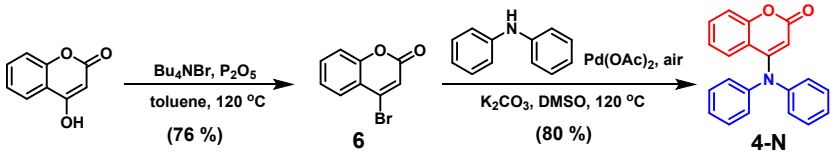

Compound 6: Following a similar procedure from literature[8], a solution of 4-hydroxy coumarin (1 g, 6.2 mmol) in toluene (40 mL) was heated to 120 °C for 10 min and then Bu_4NBr (6 g, 18.6 mmol) was added in portion-wise over 5 min, and the reaction mixture was stirred for another 10 min to dissolve the starting material completely. P_2O_5 (3.2 g, 14.9 mmol) was then added in portions over 10 min and the reaction was heated for 5 h until reaction completion by TLC monitoring (1:2 EA/petroleum ether). Then the reaction mixture was cooled to room temperature and washed with a saturated aqueous $NaHCO_3$ solution. The reaction mixture was extracted with EA, dried over anhydrous Na_2SO_4, filtered and concentrated under reduced pressure. The residue was purified by column chromatography using ethyl acetate-petroleum ether to give the desired product **7** (1.05 g, 76%).
^{1}H NMR (400 MHz, Chloroform-*d*) δ 7.86 (dd, J = 7.9, 1.6 Hz, 1H), 7.61 (ddd, J = 8.2, 7.4, 1.6 Hz, 1H), 7.45-7.32 (m, 2H), 6.88 (s, 1H).

4-N: Following a similar procedure from literature[9], a dry round-bottom flask equipped with a magnetic stirring bar was charged with diphenylamine (320 mg, 1.9 mmol), compound **7** (500 mg, 2.8 mmol), $Pd(OAc)_2$ (19 mg, 0.08 mmol) and K_2CO_3 (1 g, 2.8 mmol) in DMSO (10 mL). The reaction mixture was heated to 120 °C and stirred for overnight. After completion of the reaction by TLC monitoring (1:2 EA/petroleum ether), the reaction mixture was cooled to room temperature and added with a saturated NH_4Cl solution. Then the mixture was extracted with EA. The organic layer was dried over anhydrous Na_2SO_4, filtered and concentrated under reduced pressure. The residue was purified by column chromatography using ethyl acetate-petroleum ether to give the product **4-N**. (470 mg, 80%)
^{1}H NMR (400 MHz, Chloroform-*d*) δ 7.42 (ddd, J = 8.6, 7.1, 1.6 Hz, 1H), 7.37-7.30 (m, 4H), 7.24-7.17 (m, 3H), 7.11-7.06 (m, 3H), 6.96 (ddd, J = 8.3, 7.2, 1.4 Hz, 1H), 5.78 (s, 1H); ^{13}C NMR (101 MHz, $CDCl_3$) δ 162.38, 157.65, 154.56, 146.54, 131.40, 129.79, 126.51, 125.84, 125.70, 123.17, 117.52, 116.84, 105.08; HR-MS (ESI): m/z cal for $C_{21}H_{16}NO_2$ $[M+H]^+$: 314.1176; found: 314.1176.

2. Additional Experimental and Calculation Results

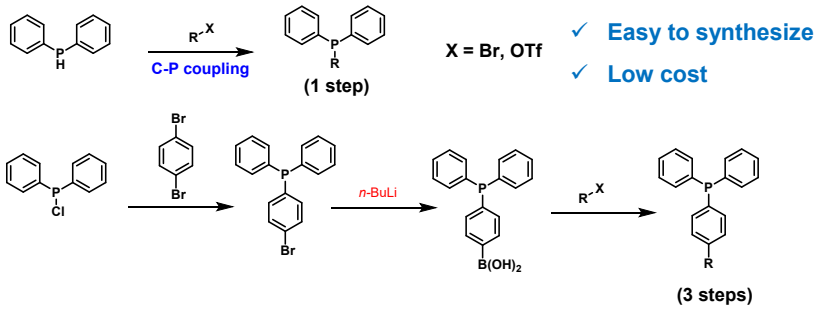

Figure S1. Comparison of the synthetic routes based on DPP modification and TPP modification. From the perspective of synthesis, DPP modification is more economical and the reaction conditions are moderate.

Table S1. Summary of the photophysical properties of DPP-modification molecules.

PLQY	4-P	7P-4Me	7P-3COMe	7P-3COOEt
THF (%)	< 0.01	< 0.01	< 0.01	0.2
Solid (%)	10.3	47.0	19.0	38.4
λ_{em} (nm)	560	460	554	603

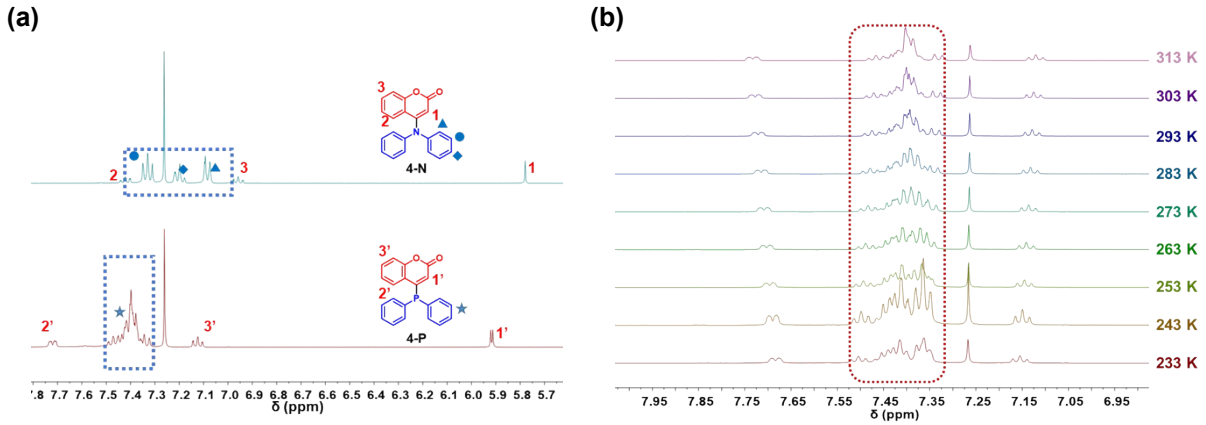

Figure S2. a) Comparison of ^{1}H NMR spectra of **4-N** and **4-P** in $CDCl_3$ at 298 K; b) ^{1}H NMR spectra of **4-P** in $CDCl_3$ at different temperatures.

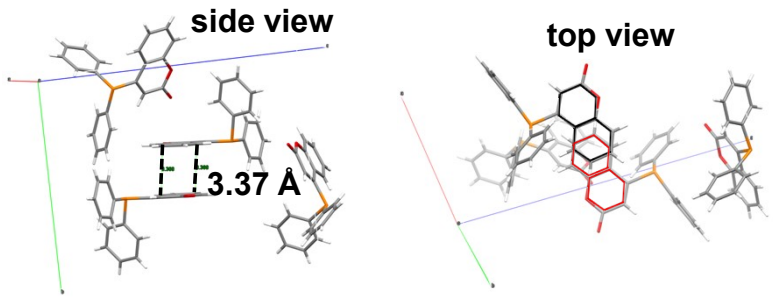

Figure S3. XRD structure analysis of **4-P** with the labelled distance between adjacent molecule layer and overlap of conjugated area.

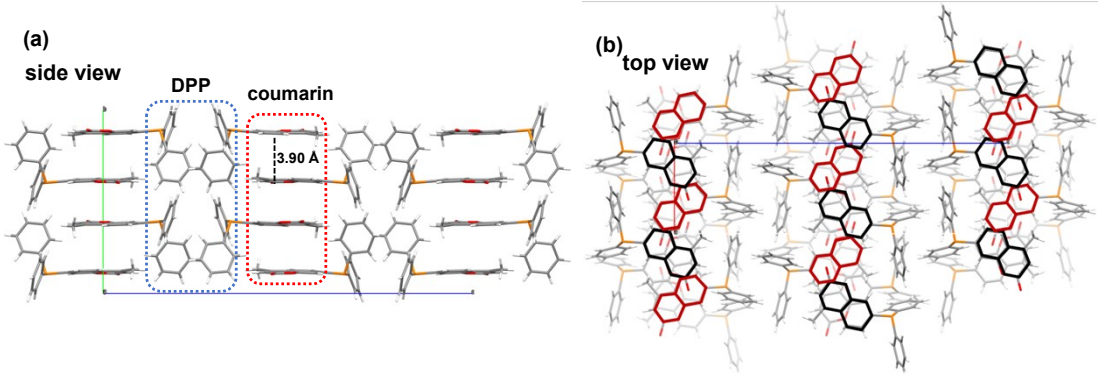

Figure S4. XRD structure analysis of **7P-4Me** with the labelled distance between adjacent molecule layer and overlap of conjugated area.

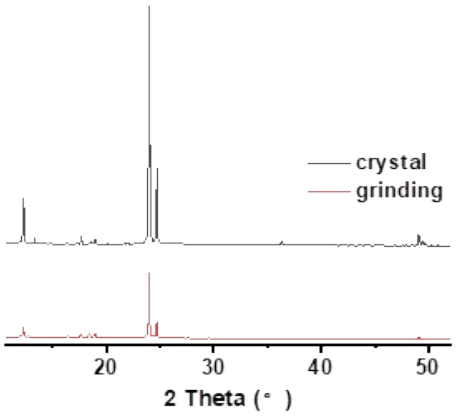

Figure S5. Powder XRD results of **7P-4Me** before and after grinding. The diffraction signals become weaker or even disappear after grinding indicating the amorphization process upon grinding.

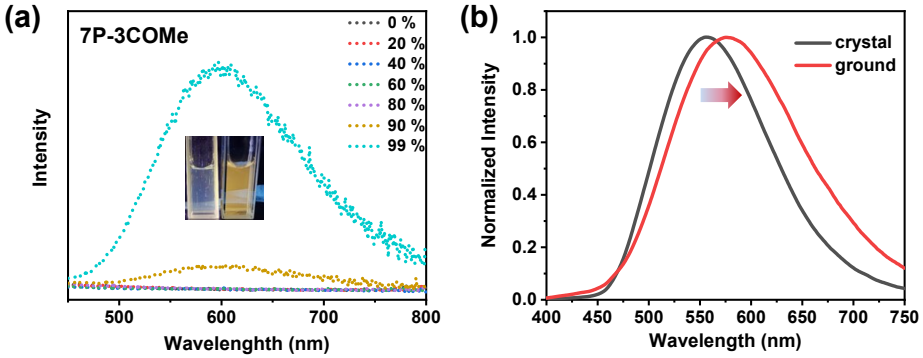

Figure S6. The emission spectra of **7P-COMe** in a) THF/H_2O mixture with different water ratios. b) crystal state before and after grinding.

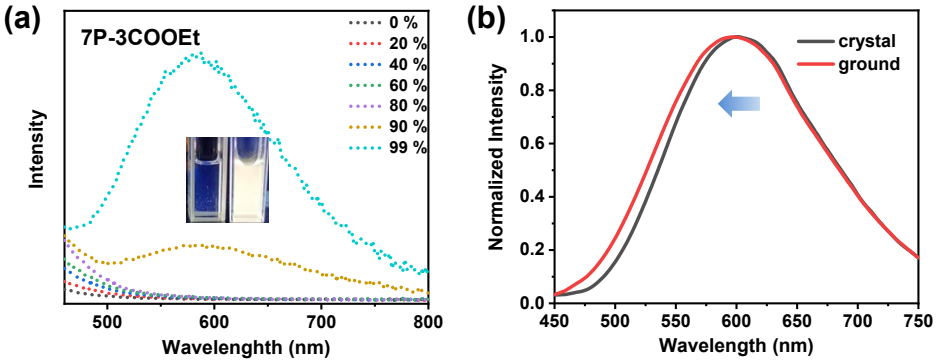

Figure S7. The emission spectra of **7P-COOEt** in a) THF/H_2O mixture with different water ratios. b) crystal state before and after grinding.

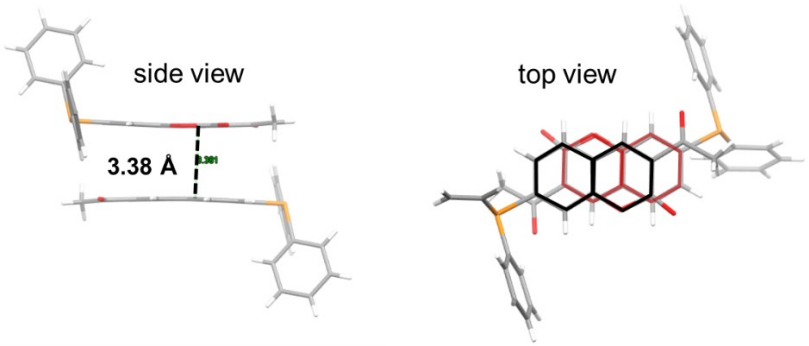

Figure S8. XRD structure analysis of **7P-COMe** with the labelled distance between adjacent molecule layer and overlap of conjugated area.

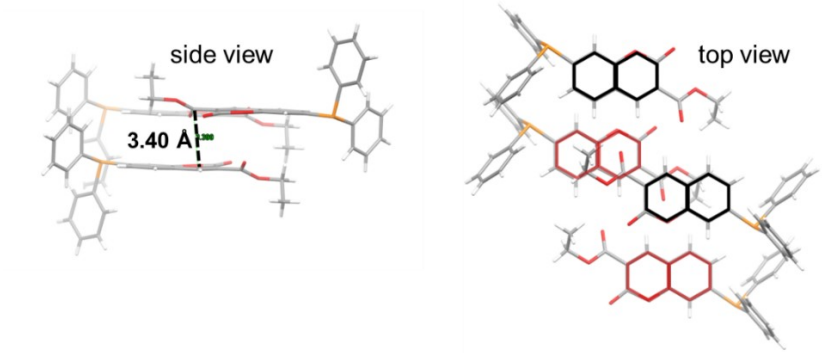

Figure S9. XRD structure analysis of **7P-COOEt** with the labelled distance between adjacent molecule layer and overlap of conjugated area.

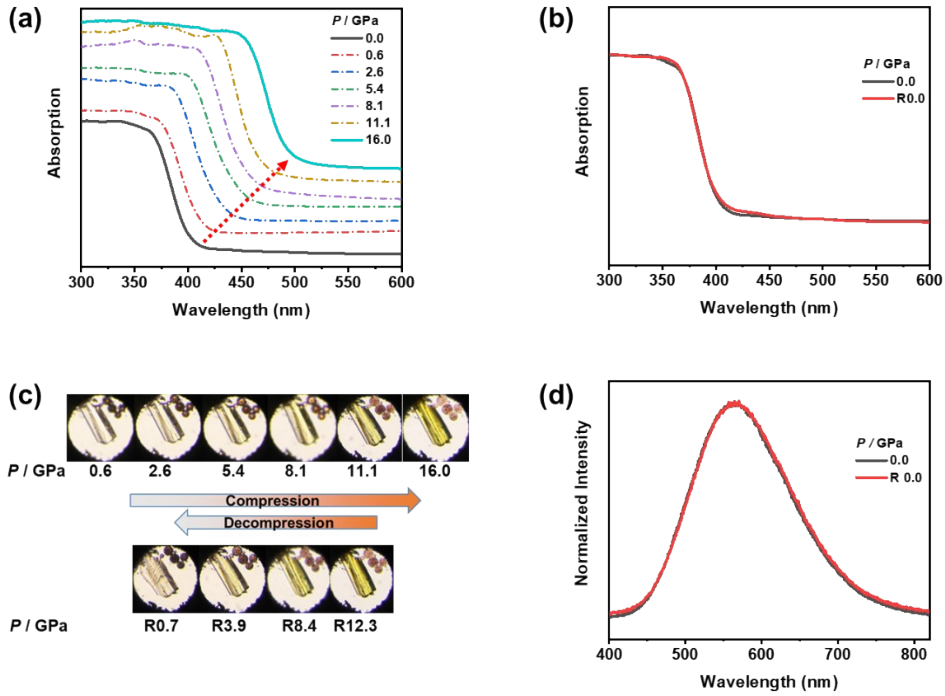

Figure S10. UV-visible absorption spectra of **4-P** crystal a) under high pressure; b) at the pressure of 0.0 GPa and released pressure of 0.0 GPa. c) Corresponding optical photographs at different pressures show the evolution of the sample's color with increasing pressure. d) PL spectra of **4-P** at the pressure of 0.0 GPa and released pressure of 0.0 GPa excited by a 355 nm laser.

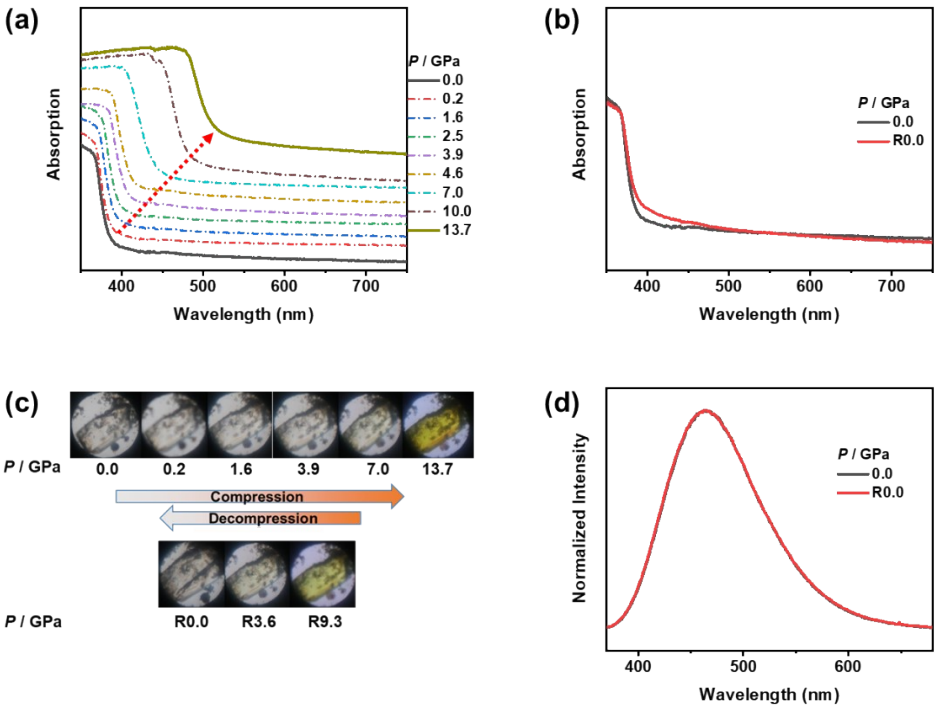

Figure S11. UV-visible absorption spectra of **7P-4Me** crystal a) under high pressure; b) at the pressure of 0.0 GPa and released pressure of 0.0 GPa. c) Corresponding optical photographs at different pressures show the evolution of the sample's color with increasing pressure. d) PL spectra of **7P-4Me** at the pressure of 0.0 GPa and released pressure of 0.0 GPa excited by a 355 nm laser.

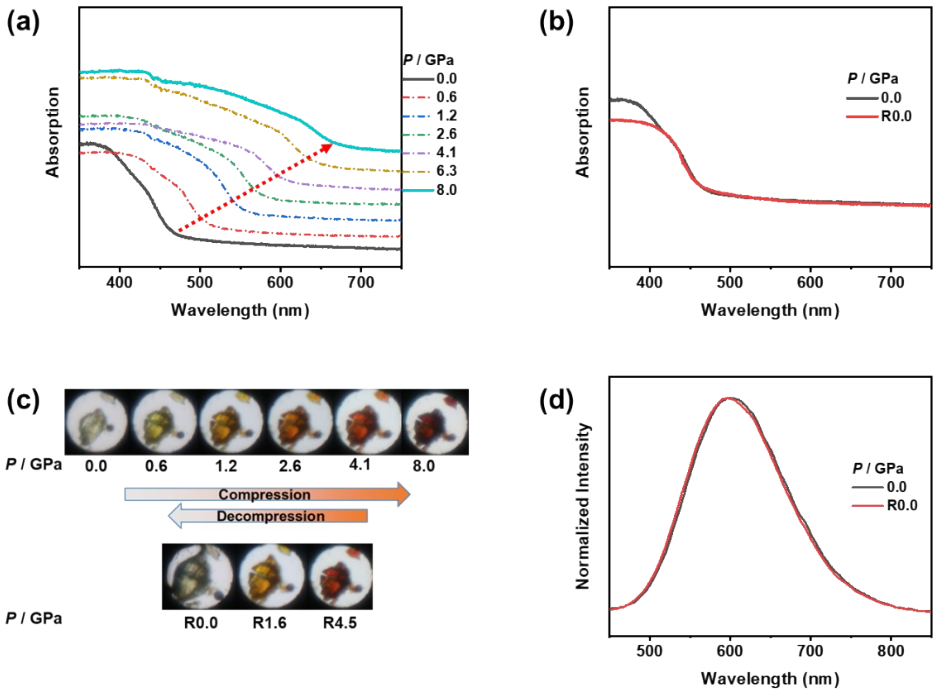

Figure S12. UV-visible absorption spectra of **7P-3COOEt** crystal a) under high pressure; b) at the pressure of 0.0 GPa and released pressure of 0.0 GPa. c) Corresponding optical photographs at different pressures show the evolution of the sample's color with increasing pressure. d) PL spectra of **7P-3COOEt** at the pressure of 0.0 GPa and released pressure of 0.0 GPa excited by a 355 nm laser.

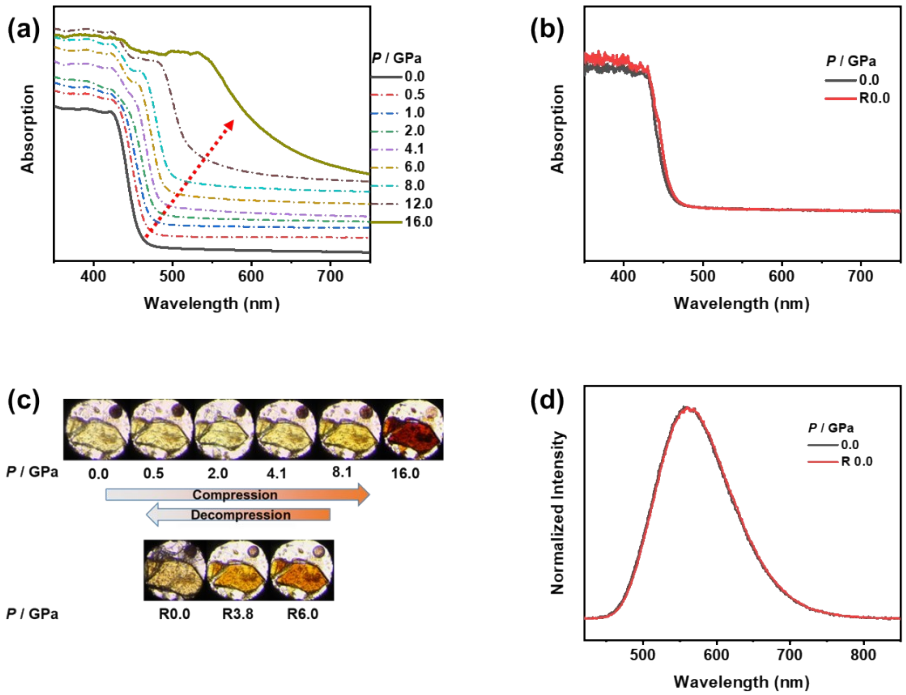

Figure S13. UV-visible absorption spectra of **7P-3COMe** crystal a) under high pressure; b) at the pressure of 0.0 GPa and released pressure of 0.0 GPa. c) Corresponding optical photographs at different pressures show the evolution of the sample's color with increasing pressure. d) PL spectra of **7P-3COMe** at the pressure of 0.0 GPa and released pressure of 0.0 GPa excited by a 355 nm laser.

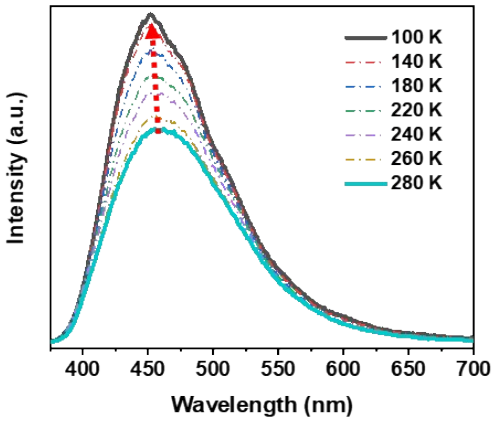

Figure S14. Temperature dependent photoluminescence spectra of **7P-4Me** in crystal state.

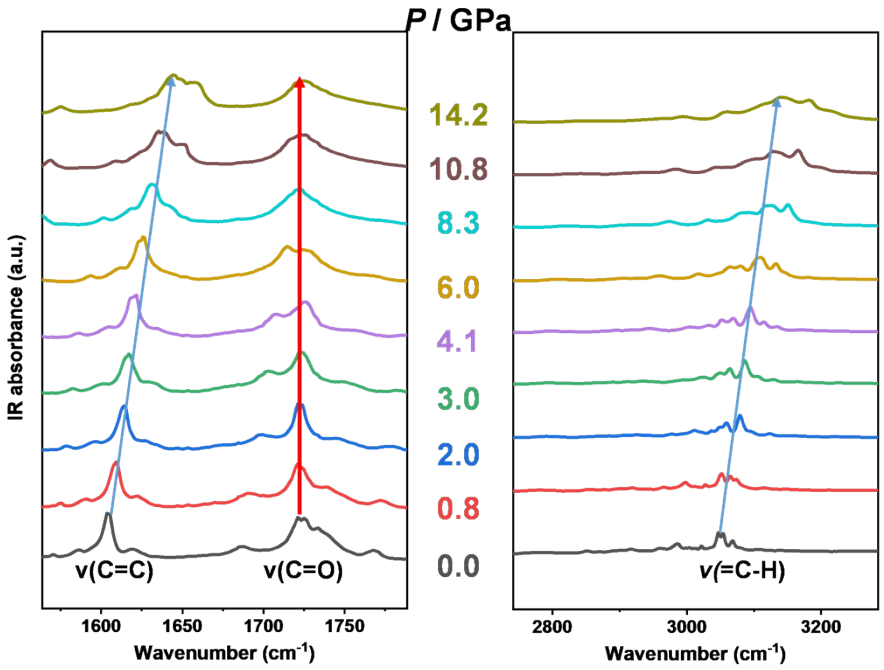

Figure S15. IR spectra of **7P-4Me** at different pressure until 14.2 GPa at room temperature in the region of *v*(C=C), *v*(C=O) and *v*(=C-H) vibrational modes. The stretching vibration frequency of carbonyl group *v*(C=O) is almost unchanged upon compression indicating that C=O bonds are not shortened with increasing pressure as observed from other bonds. This phenomena demonstrates that the C=O···H interactions get stronger with increasing pressure. The increased strength of intermolecular H-bonding hinders the intramolecular motion, therefore inhibiting the nonradiative process.

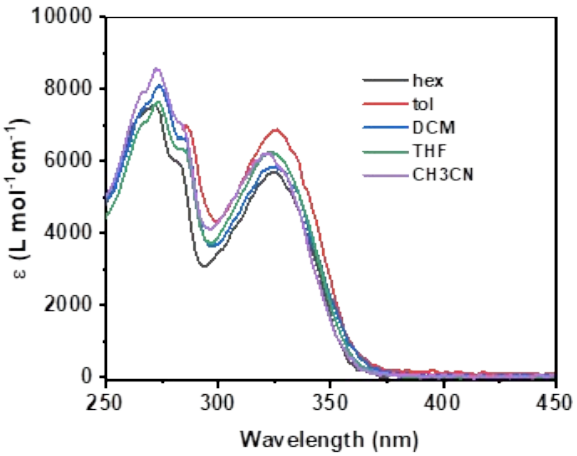

Figure S16. UV-vis spectra of **7P-4Me** in different solvents at 298 K. The absorption peaks are almost unchanged in different solvents, which indicates that it is a localized absorption.

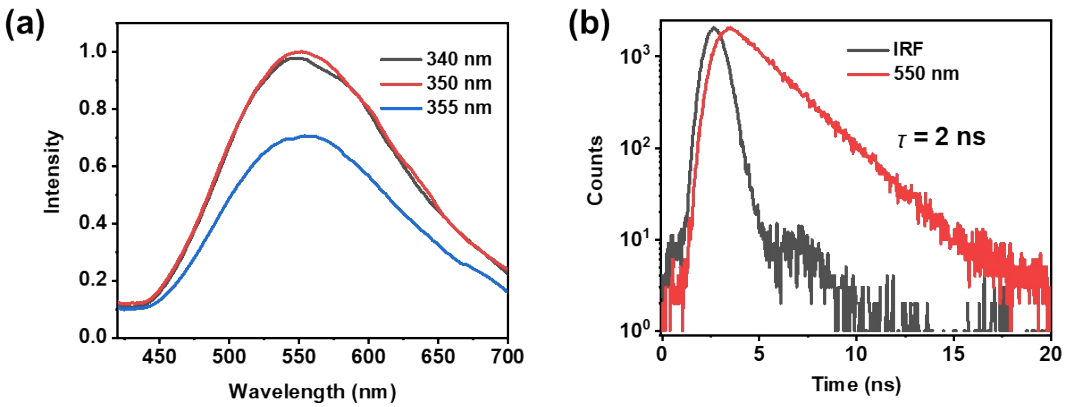

Figure S17. Emission spectra of **7P-4Me** at viable excitation wavelength and transient fluorescence decay at 550 nm in cyclohexane. The emission peak does not change under different excitation wavelength. And the emission lifetime is about 2 ns. Which means that the fluorescence emission obeys Kasha's rule.

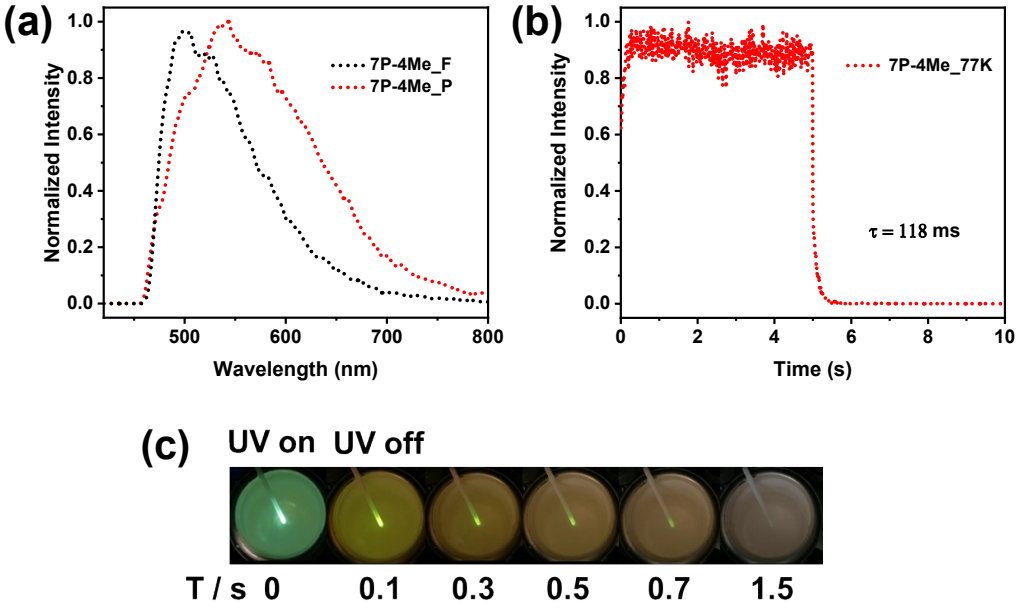

Figure S18. a) Fluorescence spectrum and phosphorescence spectrum of **7P-4Me** and b) transient phosphorescence decay curve at 550 nm in DCM under 77 K. c) Afterglow images of **7P-4Me** in DCM after 365 nm excitation at 77K.

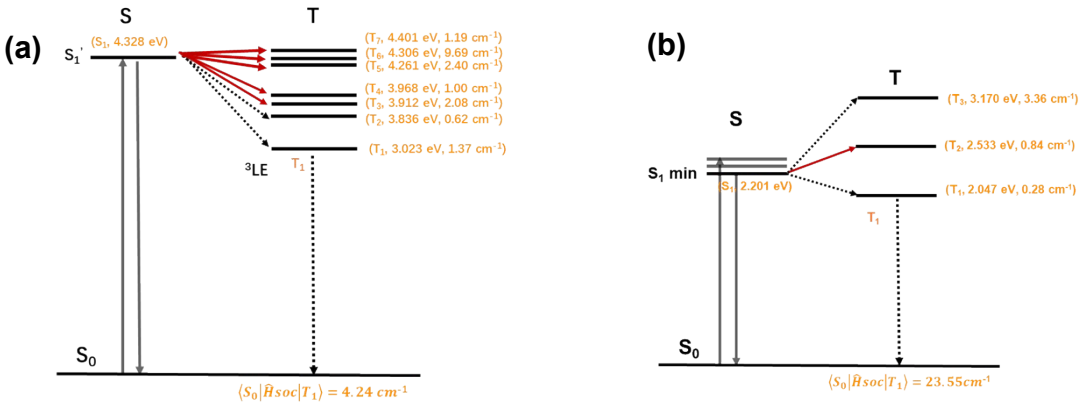

Figure S19. a) Calculated energy levels and spin-orbit coupling constants between S_1 and T_n based on the corresponding molecular geometries of $S_{0\ min}$ and $S_{1\ min}$.

3. Crystal Structures

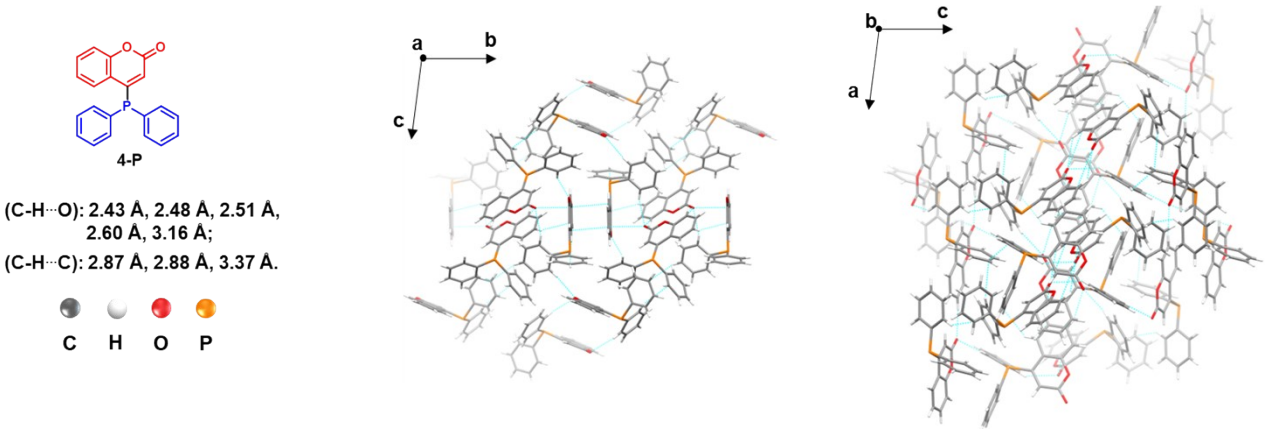

Figure S20. Crystal structure of **4-P** including the major intermolecular interactions. Color codes: C (gray), H (white), O (red), P (yellow).

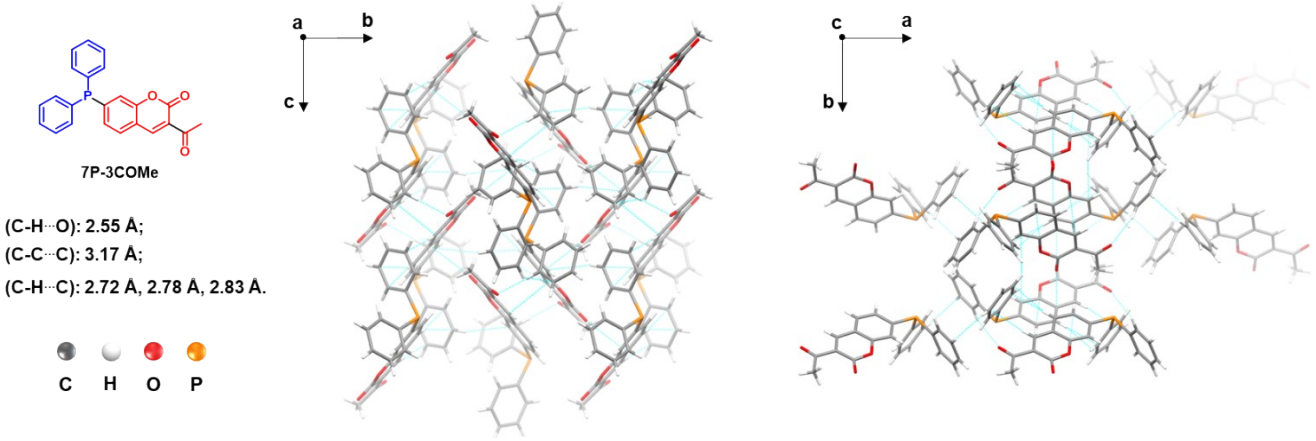

Figure S21. Crystal structure of **7P-3COMe** including the major intermolecular interactions. Color codes: C (gray), H (white), O (red), P (yellow).

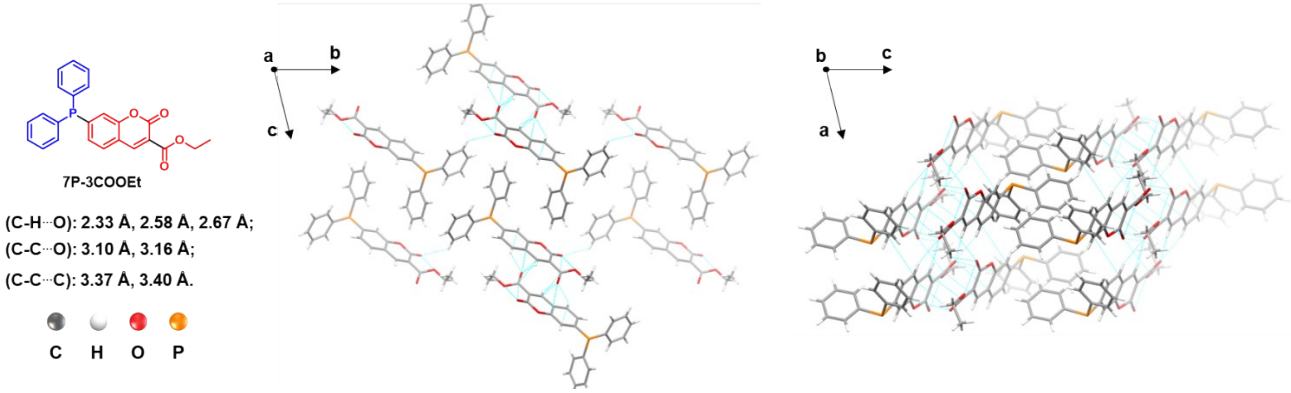

Figure S22. Crystal structure of **7P-3COOEt** including the major intermolecular interactions. Color codes: C (gray), H (white), O (red), P (yellow).

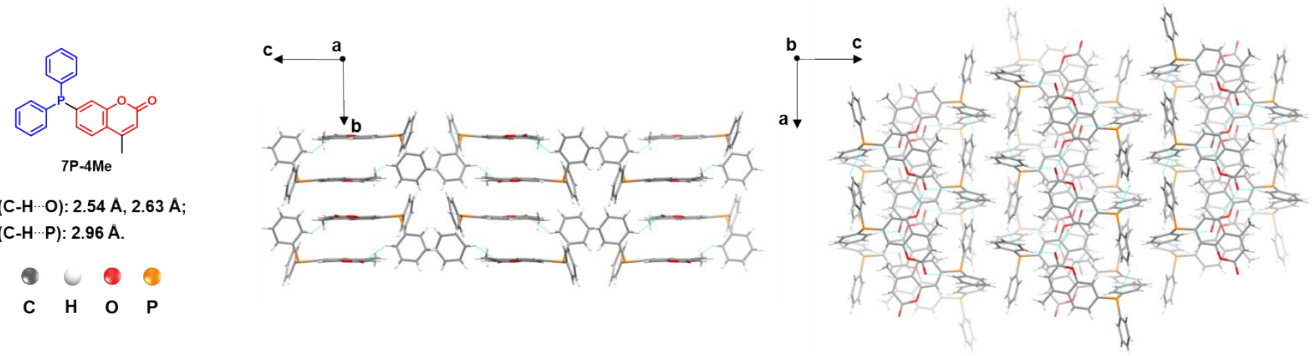

Figure S23. Crystal structure of **7P-4Me** including the major intermolecular interactions. Color codes: C (gray), H (white), O (red), P (yellow).

Table S2. Summary of the crystal structure information of DPP-modification molecules.

Identification code	4-P	7P-3COMe	7P-3COOEt	7P-4Me
CCDC number	**2119796**	**2119797**	**2119798**	**2119799**
Empirical formula	$C_{21}H_{15}O_2P$	$C_{23}H_{17}O_3P$	$C_{22}H_{17}O_2P$	$C_{22}H_{17}O_2P$
Formula weight	330.30	372.33	344.32	344.32
Temperature/K	179.99(10)	100.00(14)	100.00(11)	100.00(11)
Crystal system	triclinic	monoclinic	orthorhombic	orthorhombic
Space group	P-1	$P2_1/c$	Pbcn	Pbcn
a/Å	9.0126(2)	13.4282(9)	8.0623(2)	8.0623(2)
b/Å	14.6954(3)	13.8412(7)	14.6716(6)	14.6716(6)
c/Å	19.5545(5)	9.7598(5)	29.7285(10)	29.7285(10)
α/°	91.632(2)	90	90	90
β/°	97.805(2)	92.854(5)	90	90
γ/°	105.419(2)	90	90	90
Volume/Å³	2467.86(10)	1811.73(18)	3516.5(2)	3516.5(2)
Z	6	4	8	8
ρ_{calc}g/cm³	1.333	1.365	1.301	1.301
μ/mm⁻¹	0.176	0.173	0.168	0.168
F(000)	1032.0	776.0	1440.0	1440.0
Crystal size/mm³	0.42 × 0.03 × 0.02	0.2 × 0.1 × 0.03	0.2 × 0.02 × 0.01	0.2 × 0.02 × 0.01
Radiation	Mo Kα (λ = 0.71073)	Mo Kα (λ = 0.71073)	MoKα (λ = 0.71073)	MoKα (λ = 0.71073)
2Θ range for data collection/°	4.742 to 58.942	5.112 to 62.632	5.482 to 62.436	5.482 to 62.436
Index ranges	-10 ≤ h ≤ 12, -19 ≤ k ≤ 20, -26 ≤ l ≤ 26	-17 ≤ h ≤ 18, -12 ≤ k ≤ 19, -12 ≤ l ≤ 12	-8 ≤ h ≤ 10, -19 ≤ k ≤ 17, -41 ≤ l ≤ 30	-8 ≤ h ≤ 10, -19 ≤ k ≤ 17, -41 ≤ l ≤ 30
Reflections collected	34864	15183	16318	16318
Independent reflections	12366 [R_{int} = 0.0314, R_{sigma} = 0.0464]	4754 [R_{int} = 0.0496, R_{sigma} = 0.0609]	4601 [R_{int} = 0.0463, R_{sigma} = 0.0533]	4601 [R_{int} = 0.0463, R_{sigma} = 0.0533]
Data/restraints/parameters	12366/0/649	4754/0/245	4601/0/227	4601/0/227
Goodness-of-fit on F²	1.016	1.066	1.019	1.019
Final R indexes [I>=2σ (I)]	R_1 = 0.0446, wR_2 = 0.0986	R_1 = 0.0719, wR_2 = 0.1649	R_1 = 0.0467, wR_2 = 0.1073	R_1 = 0.0467, wR_2 = 0.1073
Final R indexes [all data]	R_1 = 0.0727, wR_2 = 0.1078	R_1 = 0.1014, wR_2 = 0.1793	R_1 = 0.0793, wR_2 = 0.1206	R_1 = 0.0793, wR_2 = 0.1206
Largest diff. peak/hole / e Å⁻³	0.28/-0.36	0.85/-0.64	0.60/-0.27	0.60/-0.27

Table S3. Fractional Atomic Coordinates (×10⁴) and Equivalent Isotropic Displacement Parameters (Å²×10³) for **4-P**. U_{eq} is defined as 1/3 of the trace of the orthogonalised U_{IJ} tensor.

Atom	*x*	*y*	*z*	U(eq)
P1	2955.8(5)	7434.9(3)	9715.0(2)	32.79(11)
O1	4054.4(15)	4409.1(9)	8742.0(7)	45.3(3)
O2	1593.0(14)	4341.2(8)	8772.7(6)	36.8(3)
C1	5072(2)	7823.2(11)	9783.7(8)	32.1(4)
C2	5870(2)	8497.4(14)	9385.5(10)	44.2(5)

C3	7478(2)	8811.3(16)	9507.9(11)	57.3(6)
C4	8314(2)	8452.7(16)	10020.8(11)	53.9(5)
C5	7545(2)	7776.5(15)	10419.4(11)	50.8(5)
C6	5942(2)	7475.7(13)	10311.7(9)	42.3(4)
C7	2253(2)	8045.4(12)	8988.1(10)	40.2(4)
C8	1977(3)	8914.2(14)	9141.7(14)	59.8(6)
C9	1362(3)	9386.1(19)	8623(2)	84.4(10)
C10	1006(3)	9005(2)	7959(2)	86.4(11)
C11	1280(3)	8157(2)	7791.7(14)	70.9(8)
C12	1919(2)	7679.2(16)	8307.7(11)	51.0(5)
C13	2460.1(18)	6225.2(11)	9322.0(8)	26.5(3)
C14	3535(2)	5801.0(11)	9158.7(8)	30.8(4)
C15	3135(2)	4828.0(12)	8885.7(9)	32.9(4)
C16	459.5(19)	4749.6(12)	8932.8(8)	31.8(4)
C17	836.7(19)	5678.2(11)	9217.6(8)	28.5(3)
C18	-392(2)	6019.0(13)	9381.7(9)	36.5(4)
C19	-1904(2)	5456.3(15)	9258.6(9)	44.3(5)
C20	-2234(2)	4541.7(16)	8959.8(10)	46.2(5)
C21	-1055(2)	4183.9(14)	8798.4(9)	41.5(4)
P2	1618.5(5)	3883.4(3)	6577.5(2)	26.74(10)
O3	-1493.2(14)	3589.5(10)	4109.8(6)	47.2(3)
O4	974.5(12)	3625.9(8)	4173.1(5)	30.6(2)
C22	-310.5(19)	3845.2(11)	6785.6(8)	29.0(3)
C23	-605(2)	4716.2(13)	6908.8(9)	38.4(4)
C24	-2007(2)	4761.9(15)	7095.0(9)	47.8(5)
C25	-3130(2)	3941.6(16)	7170.1(9)	46.2(5)
C26	-2860(2)	3074.3(15)	7050.9(9)	45.2(5)
C27	-1461(2)	3023.7(13)	6853.7(9)	37.8(4)
C28	1854.2(18)	2710.6(11)	6760.5(8)	26.2(3)
C29	2651(2)	2621.8(12)	7409.2(8)	33.3(4)
C30	2958(2)	1771.6(14)	7569.0(9)	41.9(4)
C31	2487(2)	1009.3(13)	7088.4(10)	40.0(4)
C32	1682(2)	1081.9(12)	6449.5(9)	37.4(4)
C33	1361(2)	1927.7(11)	6285.9(9)	32.3(4)
C34	1302.4(18)	3766.6(10)	5625.2(8)	24.7(3)
C35	-70.5(18)	3718.6(11)	5234.5(8)	30.8(4)
C36	-286.7(19)	3643.2(12)	4485.6(9)	32.7(4)
C37	2405.4(18)	3692.1(10)	4556.1(8)	25.4(3)
C38	2634.1(17)	3775.1(10)	5276.1(8)	23.9(3)
C39	4137.3(18)	3863.4(11)	5618.0(9)	28.9(3)
C40	5343.0(19)	3871.9(11)	5252.0(9)	32.4(4)
C41	5082(2)	3784.8(11)	4535.7(9)	32.8(4)
C42	3605.2(19)	3690.7(11)	4181.9(9)	30.5(4)
P3	4795.8(5)	847.1(3)	3037.7(2)	25.41(10)
O5	900.0(15)	1493.5(8)	4574.6(7)	42.6(3)
O6	1731.2(13)	234.2(8)	4785.7(6)	32.1(3)
C43	3630.4(18)	-66.9(10)	2374.3(8)	25.8(3)
C44	2077(2)	-560.1(11)	2373.9(9)	33.5(4)
C45	1295(2)	-1239.3(12)	1850.5(9)	39.3(4)
C46	2047(2)	-1436.4(12)	1317.2(9)	39.2(4)
C47	3590(2)	-953.2(13)	1310.7(9)	39.8(4)
C48	4374(2)	-280.0(12)	1836.4(8)	32.0(4)
C49	4449.7(18)	1929.2(10)	2693.0(8)	25.8(3)
C50	5625(2)	2763.4(11)	2874.3(8)	32.9(4)
C51	5469(2)	3612.6(12)	2625.2(10)	40.0(4)
C52	4154(2)	3639.3(12)	2188.9(9)	38.8(4)
C53	2974(2)	2820.4(13)	2007.7(10)	43.3(4)
C54	3123(2)	1968.8(12)	2256.6(9)	37.2(4)
C55	3543.4(17)	621.4(10)	3715.3(8)	24.3(3)
C56	2661.1(19)	1187.3(11)	3867.5(8)	28.3(3)
C57	1716.4(19)	1014.4(11)	4418.8(9)	30.8(4)
C58	2635.0(18)	-356.7(10)	4647.9(8)	26.5(3)
C59	3565.3(17)	-187.5(10)	4126.7(8)	24.5(3)
C60	4482.0(19)	-806.2(11)	4039.6(8)	28.6(3)
C61	4451.8(19)	-1549.5(11)	4453.6(9)	31.5(4)
C62	3495(2)	-1705.2(11)	4962.6(9)	32.5(4)
C63	2576.7(19)	-1110.3(11)	5063.1(8)	31.0(4)

Table S4. Bond Lengths for **4-P**.

Atom	Atom	Length/Å	Atom	Atom	Length/Å
P1	C1	1.8245(18)	C29	C30	1.385(2)
P1	C13	1.8321(16)	C30	C31	1.377(3)
P1	C7	1.8321(19)	C31	C32	1.379(3)

O1	C15	1.212(2)	C32	C33	1.385(2)
O2	C15	1.368(2)	C34	C35	1.347(2)
O2	C16	1.380(2)	C34	C38	1.457(2)
C1	C2	1.387(2)	C35	C36	1.448(2)
C1	C6	1.402(2)	C37	C42	1.386(2)
C2	C3	1.384(3)	C37	C38	1.392(2)
C3	C4	1.374(3)	C38	C39	1.398(2)
C4	C5	1.378(3)	C39	C40	1.378(2)
C5	C6	1.378(3)	C40	C41	1.385(2)
C7	C12	1.384(3)	C41	C42	1.384(2)
C7	C8	1.396(3)	P3	C49	1.8297(16)
C8	C9	1.382(4)	P3	C55	1.8362(15)
C9	C10	1.361(4)	P3	C43	1.8360(16)
C10	C11	1.372(4)	O5	C57	1.2058(19)
C11	C12	1.393(3)	O6	C57	1.3718(19)
C13	C14	1.350(2)	O6	C58	1.3830(18)
C13	C17	1.453(2)	C43	C48	1.392(2)
C14	C15	1.446(2)	C43	C44	1.395(2)
C16	C21	1.382(2)	C44	C45	1.383(2)
C16	C17	1.395(2)	C45	C46	1.382(3)
C17	C18	1.400(2)	C46	C47	1.385(3)
C18	C19	1.378(3)	C47	C48	1.381(2)
C19	C20	1.390(3)	C49	C54	1.387(2)
C20	C21	1.372(3)	C49	C50	1.391(2)
P2	C22	1.8256(17)	C50	C51	1.387(2)
P2	C28	1.8311(16)	C51	C52	1.373(3)
P2	C34	1.8413(15)	C52	C53	1.378(3)
O3	C36	1.209(2)	C53	C54	1.388(2)
O4	C36	1.3672(19)	C55	C56	1.347(2)
O4	C37	1.3785(19)	C55	C59	1.457(2)
C22	C27	1.390(2)	C56	C57	1.450(2)
C22	C23	1.395(2)	C58	C63	1.386(2)
C23	C24	1.379(3)	C58	C59	1.393(2)
C24	C25	1.379(3)	C59	C60	1.402(2)
C25	C26	1.379(3)	C60	C61	1.375(2)
C26	C27	1.387(2)	C61	C62	1.389(2)
C28	C33	1.392(2)	C62	C63	1.381(2)
C28	C29	1.398(2)			

Table S5. Bond Angles for **4-P.**

Atom	Atom	Atom	Angle/°	Atom	Atom	Atom	Angle/°
C1	P1	C13	103.39(7)	C32	C33	C28	120.53(15)
C1	P1	C7	104.65(8)	C35	C34	C38	118.27(14)
C13	P1	C7	100.59(8)	C35	C34	P2	123.70(12)
C15	O2	C16	121.54(13)	C38	C34	P2	117.96(11)
C2	C1	C6	118.03(17)	C34	C35	C36	122.79(15)
C2	C1	P1	124.12(14)	O3	C36	O4	116.86(15)
C6	C1	P1	117.63(13)	O3	C36	C35	125.60(16)
C3	C2	C1	120.60(18)	O4	C36	C35	117.54(14)
C4	C3	C2	120.61(19)	O4	C37	C42	116.05(14)
C3	C4	C5	119.8(2)	O4	C37	C38	121.80(13)
C6	C5	C4	120.03(19)	C42	C37	C38	122.14(15)
C5	C6	C1	120.94(17)	C37	C38	C39	117.55(14)
C12	C7	C8	118.6(2)	C37	C38	C34	118.27(14)
C12	C7	P1	124.06(14)	C39	C38	C34	124.18(14)
C8	C7	P1	117.27(17)	C40	C39	C38	120.88(16)
C9	C8	C7	120.3(3)	C39	C40	C41	120.37(16)
C10	C9	C8	120.4(3)	C42	C41	C40	120.16(15)
C9	C10	C11	120.6(2)	C41	C42	C37	118.90(15)
C10	C11	C12	119.7(3)	C49	P3	C55	102.59(7)
C7	C12	C11	120.5(2)	C49	P3	C43	102.36(7)
C14	C13	C17	118.42(14)	C55	P3	C43	99.47(7)
C14	C13	P1	123.26(13)	C57	O6	C58	121.62(12)
C17	C13	P1	118.23(12)	C48	C43	C44	118.27(15)
C13	C14	C15	122.69(16)	C48	C43	P3	116.73(12)
O1	C15	O2	117.16(15)	C44	C43	P3	125.01(12)
O1	C15	C14	125.35(16)	C45	C44	C43	120.81(16)
O2	C15	C14	117.49(15)	C46	C45	C44	120.15(17)
O2	C16	C21	116.10(16)	C45	C46	C47	119.70(16)
O2	C16	C17	121.42(15)	C48	C47	C46	120.12(16)
C21	C16	C17	122.48(17)	C47	C48	C43	120.93(16)
C16	C17	C18	117.12(16)	C54	C49	C50	118.32(15)
C16	C17	C13	118.38(15)	C54	C49	P3	124.71(12)

C18	C17	C13	124.51(15)	C50	C49	P3	116.95(12)
C19	C18	C17	120.86(18)	C51	C50	C49	120.68(16)
C18	C19	C20	120.22(18)	C52	C51	C50	120.33(16)
C21	C20	C19	120.35(18)	C51	C52	C53	119.74(16)
C20	C21	C16	118.96(19)	C52	C53	C54	120.13(17)
C22	P2	C28	104.32(7)	C49	C54	C53	120.79(16)
C22	P2	C34	103.09(7)	C56	C55	C59	118.73(14)
C28	P2	C34	99.80(7)	C56	C55	P3	123.24(12)
C36	O4	C37	121.28(12)	C59	C55	P3	117.97(11)
C27	C22	C23	118.58(16)	C55	C56	C57	122.48(14)
C27	C22	P2	124.98(13)	O5	C57	O6	117.29(14)
C23	C22	P2	116.39(13)	O5	C57	C56	125.27(15)
C24	C23	C22	120.77(18)	O6	C57	C56	117.43(14)
C23	C24	C25	120.04(18)	O6	C58	C63	116.26(14)
C26	C25	C24	120.03(18)	O6	C58	C59	121.33(13)
C25	C26	C27	120.18(19)	C63	C58	C59	122.40(14)
C26	C27	C22	120.38(17)	C58	C59	C60	117.33(14)
C33	C28	C29	118.78(14)	C58	C59	C55	118.37(14)
C33	C28	P2	124.19(12)	C60	C59	C55	124.29(14)
C29	C28	P2	116.95(12)	C61	C60	C59	120.90(15)
C30	C29	C28	120.22(16)	C60	C61	C62	120.26(15)
C31	C30	C29	120.22(16)	C63	C62	C61	120.42(15)
C30	C31	C32	120.25(16)	C62	C63	C58	118.67(15)
C31	C32	C33	119.99(16)				

Table S6. Fractional Atomic Coordinates (×10^4) and Equivalent Isotropic Displacement Parameters (Å^2×10^3) for **7P-4Me**. Ueq is defined as 1/3 of the trace of the orthogonalised UIJ tensor.

Atom	*x*	*y*	*z*	U(eq)
P11	5865.9(5)	6061.4(3)	6547.6(2)	15.16(12)
O1	9417.7(14)	6110.2(10)	5136.4(4)	22.3(3)
O24	11223.7(15)	6057.3(11)	4576.3(5)	30.8(4)
C12	6470.1(19)	7204.7(12)	6731.5(6)	14.7(3)
C2	7799(2)	6154.8(13)	5290.2(6)	17.5(4)
C13	6636(2)	7954.6(13)	6444.8(6)	17.3(4)
C18	3638(2)	6039.3(12)	6663.2(6)	15.3(3)
C15	7611(2)	8873.5(13)	7061.0(6)	19.2(4)
C16	7451(2)	8138.8(13)	7347.3(6)	20.3(4)
C4	5996(2)	6160.6(12)	5934.2(6)	16.7(3)
C23	3000(2)	5220.9(13)	6826.1(6)	19.3(4)
C7	6458(2)	6222.3(12)	4991.3(6)	17.3(4)
C3	7590(2)	6117.4(13)	5750.0(6)	17.3(4)
C5	4633(2)	6224.1(13)	5641.4(6)	19.6(4)
C17	6891(2)	7305.1(13)	7186.7(6)	18.2(4)
C21	289(2)	5886.4(14)	6885.1(6)	21.3(4)
C14	7196(2)	8784.5(13)	6608.9(6)	18.8(4)
C22	1321(2)	5143.6(14)	6935.0(6)	23.1(4)
C20	903(2)	6706.8(13)	6722.5(6)	19.9(4)
C19	2573(2)	6783.7(13)	6611.4(6)	18.3(4)
C6	4859(2)	6254.1(13)	5180.1(6)	20.4(4)
C10	9774(2)	6102.3(14)	4681.0(6)	23.1(4)
C8	6795(2)	6228.2(13)	4510.8(6)	19.2(4)
C9	8384(2)	6156.8(14)	4373.8(6)	23.0(4)
C25	5382(2)	6321.7(15)	4185.7(6)	24.9(4)

Table S7. Bond Lengths for **7P-4Me.**

Atom	Atom	Length/Å	Atom	Atom	Length/Å
P11	C12	1.8303(18)	C15	C14	1.391(2)
P11	C18	1.8290(17)	C16	C17	1.389(3)
P11	C4	1.8323(18)	C4	C3	1.399(2)
O1	C2	1.3847(19)	C4	C5	1.405(2)
O1	C10	1.384(2)	C23	C22	1.397(2)
O24	C10	1.212(2)	C7	C6	1.406(2)
C12	C13	1.398(2)	C7	C8	1.454(2)
C12	C17	1.403(2)	C5	C6	1.384(3)
C2	C7	1.403(2)	C21	C22	1.379(3)
C2	C3	1.378(2)	C21	C20	1.388(3)
C13	C14	1.387(3)	C20	C19	1.391(2)
C18	C23	1.393(3)	C10	C9	1.448(3)
C18	C19	1.398(2)	C8	C9	1.348(2)
C15	C16	1.379(3)	C8	C25	1.500(2)

Table S8. Bond Angles for **7P-4Me.**

Atom	Atom	Atom	Angle/°	Atom	Atom	Atom	Angle/°
C12	P11	C4	102.08(8)	C2	C7	C6	117.12(16)
C18	P11	C12	102.80(8)	C2	C7	C8	118.59(15)
C18	P11	C4	104.15(7)	C6	C7	C8	124.26(16)
C10	O1	C2	121.26(14)	C2	C3	C4	119.92(16)
C13	C12	P11	124.38(14)	C6	C5	C4	120.87(16)
C13	C12	C17	118.84(16)	C16	C17	C12	120.18(17)
C17	C12	P11	116.65(13)	C22	C21	C20	120.51(16)
O1	C2	C7	121.38(16)	C13	C14	C15	120.02(17)
C3	C2	O1	116.14(15)	C21	C22	C23	119.71(18)
C3	C2	C7	122.47(15)	C21	C20	C19	119.87(17)
C14	C13	C12	120.50(16)	C20	C19	C18	120.34(17)
C23	C18	P11	116.32(13)	C5	C6	C7	120.99(16)
C23	C18	C19	118.99(15)	O1	C10	C9	117.14(15)
C19	C18	P11	124.66(14)	O24	C10	O1	116.87(16)
C16	C15	C14	120.02(17)	O24	C10	C9	125.99(17)
C15	C16	C17	120.44(16)	C7	C8	C25	119.44(15)
C3	C4	P11	116.02(13)	C9	C8	C7	118.30(16)
C3	C4	C5	118.61(16)	C9	C8	C25	122.25(17)
C5	C4	P11	125.27(13)	C8	C9	C10	123.29(17)
C18	C23	C22	120.57(17)				

Table S9. Fractional Atomic Coordinates ($\times 10^4$) and Equivalent Isotropic Displacement Parameters ($Å^2 \times 10^3$) for **7P-3COMe.** Ueq is defined as 1/3 of the trace of the orthogonalised UIJ tensor.

Atom	*x*	*y*	*z*	U(eq)
P11	7984.1(5)	5101.1(5)	3816.1(7)	18.85(18)
O10	5729.9(13)	3317.1(13)	134.1(18)	20.9(4)
O25	2183.3(14)	3616.0(14)	-268(2)	28.6(5)
O27	4917.7(15)	2414.6(15)	-1401(2)	35.3(5)
C12	7803.1(19)	4538.2(18)	5485(3)	18.9(5)
C23	9140.1(19)	4471.7(19)	1715(3)	20.8(5)
C2	6703.9(18)	4163.9(17)	1807(3)	18.2(5)
C6	4906.8(18)	4410.2(17)	1631(2)	17.5(5)
C18	8836.2(18)	4249.1(17)	3039(3)	17.8(5)
C8	3928.0(18)	3465.9(17)	-56(3)	18.4(5)
C5	4999(2)	5067.0(18)	2736(3)	21.7(5)
C1	5772.5(18)	3977.8(17)	1190(2)	17.6(5)
C24	2909.6(19)	3197.6(19)	-668(3)	22.0(5)
C3	6790.8(19)	4801.6(17)	2907(3)	18.9(5)
C22	9781(2)	3860.7(19)	1050(3)	22.7(5)
C13	8345.7(19)	4929.1(18)	6617(3)	20.7(5)
C17	7176.5(19)	3746.5(17)	5683(3)	19.9(5)
C9	4838.6(19)	3012.6(18)	-519(3)	21.4(5)
C16	7101(2)	3349.8(18)	6987(3)	21.2(5)
C4	5922(2)	5259.2(19)	3352(3)	22.2(5)
C7	3978.8(18)	4132.8(18)	962(3)	19.2(5)
C15	7663(2)	3733.4(19)	8102(3)	22.4(5)
C19	9220(2)	3417.2(19)	3683(3)	22.8(5)
C20	9877(2)	2818.5(19)	3022(3)	24.3(6)
C21	10152.6(19)	3032.0(19)	1704(3)	22.8(5)
C14	8279(2)	4521(2)	7913(3)	23.9(6)
C26	2806(2)	2427(2)	-1747(3)	34.6(7)

Table S10. Bond Angles for **7P-3COMe**.

Atom	Atom	Atom	Angle/°	Atom	Atom	Atom	Angle/°
C12	P11	C18	101.96(11)	C2	C1	C6	122.3(2)
C12	P11	C3	100.47(11)	O25	C24	C8	118.7(2)
C18	P11	C3	101.67(11)	O25	C24	C26	121.1(2)
C1	O10	C9	123.1(2)	C26	C24	C8	120.1(2)
C13	C12	P11	116.73(19)	C2	C3	P11	123.57(19)
C17	C12	P11	124.21(19)	C2	C3	C4	118.8(2)
C17	C12	C13	119.1(2)	C4	C3	P11	117.58(19)
C22	C23	C18	120.6(2)	C23	C22	C21	120.2(2)
C1	C2	C3	119.5(2)	C14	C13	C12	120.3(2)
C5	C6	C7	124.3(2)	C16	C17	C12	120.3(2)
C1	C6	C5	118.0(2)	O10	C9	C8	116.2(2)
C1	C6	C7	117.7(2)	O27	C9	O10	115.5(2)
C23	C18	P11	117.00(19)	O27	C9	C8	128.3(2)

C19	C18	P11	124.6(2)	C17	C16	C15	120.0(2)
C19	C18	C23	118.4(2)	C5	C4	C3	121.2(2)
C9	C8	C24	121.7(2)	C8	C7	C6	121.9(2)
C7	C8	C24	117.9(2)	C14	C15	C16	119.8(2)
C7	C8	C9	120.3(2)	C20	C19	C18	120.7(2)
C4	C5	C6	120.1(2)	C21	C20	C19	120.5(2)
O10	C1	C2	116.9(2)	C20	C21	C22	119.6(3)
O10	C1	C6	120.8(2)	C15	C14	C13	120.4(2)

Table S11. Fractional Atomic Coordinates (×10⁴) and Equivalent Isotropic Displacement Parameters (Å²×10³) for **7P-3COOEt**. Ueq is defined as 1/3 of the trace of the orthogonalised UIJ tensor.

Atom	*x*	*y*	*z*	U(eq)
P11	5865.9(5)	6061.4(3)	6547.6(2)	15.16(12)
O1	9417.7(14)	6110.2(10)	5136.4(4)	22.3(3)
O24	11223.7(15)	6057.3(11)	4576.3(5)	30.8(4)
C12	6470.1(19)	7204.7(12)	6731.5(6)	14.7(3)
C2	7799(2)	6154.8(13)	5290.2(6)	17.5(4)
C13	6636(2)	7954.6(13)	6444.8(6)	17.3(4)
C18	3638(2)	6039.3(12)	6663.2(6)	15.3(3)
C15	7611(2)	8873.5(13)	7061.0(6)	19.2(4)
C16	7451(2)	8138.8(13)	7347.3(6)	20.3(4)
C4	5996(2)	6160.6(12)	5934.2(6)	16.7(3)
C23	3000(2)	5220.9(13)	6826.1(6)	19.3(4)
C7	6458(2)	6222.3(12)	4991.3(6)	17.3(4)
C3	7590(2)	6117.4(13)	5750.0(6)	17.3(4)
C5	4633(2)	6224.1(13)	5641.4(6)	19.6(4)
C17	6891(2)	7305.1(13)	7186.7(6)	18.2(4)
C21	289(2)	5886.4(14)	6885.1(6)	21.3(4)
C14	7196(2)	8784.5(13)	6608.9(6)	18.8(4)
C22	1321(2)	5143.6(14)	6935.0(6)	23.1(4)
C20	903(2)	6706.8(13)	6722.5(6)	19.9(4)
C19	2573(2)	6783.7(13)	6611.4(6)	18.3(4)
C6	4859(2)	6254.1(13)	5180.1(6)	20.4(4)
C10	9774(2)	6102.3(14)	4681.0(6)	23.1(4)
C8	6795(2)	6228.2(13)	4510.8(6)	19.2(4)
C9	8384(2)	6156.8(14)	4373.8(6)	23.0(4)
C25	5382(2)	6321.7(15)	4185.7(6)	24.9(4)

Table S12. Bond Lengths for **7P-3COOEt.**

Atom	Atom	Length/Å	Atom	Atom	Length/Å
P11	C12	1.8303(18)	C15	C14	1.391(2)
P11	C18	1.8290(17)	C16	C17	1.389(3)
P11	C4	1.8323(18)	C4	C3	1.399(2)
O1	C2	1.3847(19)	C4	C5	1.405(2)
O1	C10	1.384(2)	C23	C22	1.397(2)
O24	C10	1.212(2)	C7	C6	1.406(2)
C12	C13	1.398(2)	C7	C8	1.454(2)
C12	C17	1.403(2)	C5	C6	1.384(3)
C2	C7	1.403(2)	C21	C22	1.379(3)
C2	C3	1.378(2)	C21	C20	1.388(3)
C13	C14	1.387(3)	C20	C19	1.391(2)
C18	C23	1.393(3)	C10	C9	1.448(3)
C18	C19	1.398(2)	C8	C9	1.348(2)
C15	C16	1.379(3)	C8	C25	1.500(2)

Table S13. Bond Angles for **7P-3COOEt**.

Atom	Atom	Atom	Angle/°	Atom	Atom	Atom	Angle/°
C12	P11	C4	102.08(8)	C2	C7	C6	117.12(16)
C18	P11	C12	102.80(8)	C2	C7	C8	118.59(15)
C18	P11	C4	104.15(7)	C6	C7	C8	124.26(16)
C10	O1	C2	121.26(14)	C2	C3	C4	119.92(16)
C13	C12	P11	124.38(14)	C6	C5	C4	120.87(16)
C13	C12	C17	118.84(16)	C16	C17	C12	120.18(17)
C17	C12	P11	116.65(13)	C22	C21	C20	120.51(16)
O1	C2	C7	121.38(16)	C13	C14	C15	120.02(17)
C3	C2	O1	116.14(15)	C21	C22	C23	119.71(18)
C3	C2	C7	122.47(15)	C21	C20	C19	119.87(17)
C14	C13	C12	120.50(16)	C20	C19	C18	120.34(17)
C23	C18	P11	116.32(13)	C5	C6	C7	120.99(16)
C23	C18	C19	118.99(15)	O1	C10	C9	117.14(15)

C19	C18	P11	124.66(14)	O24	C10	O1	116.87(16)
C16	C15	C14	120.02(17)	O24	C10	C9	125.99(17)
C15	C16	C17	120.44(16)	C7	C8	C25	119.44(15)
C3	C4	P11	116.02(13)	C9	C8	C7	118.30(16)
C3	C4	C5	118.61(16)	C9	C8	C25	122.25(17)
C5	C4	P11	125.27(13)	C8	C9	C10	123.29(17)
C18	C23	C22	120.57(17)				

4. Discussion on the Stability of DPP-modified AIEgens.

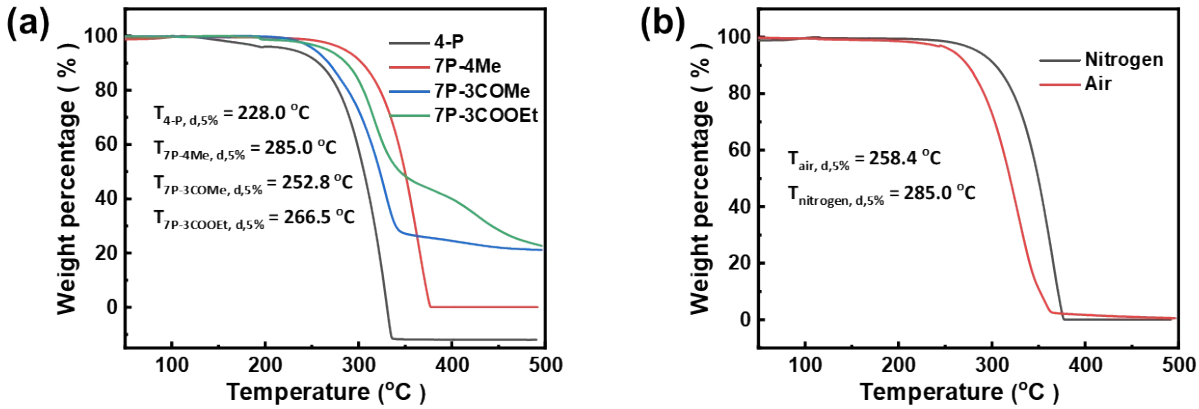

Figure S24. Thermostability of **4-P**, **7P-4Me**, **7P-3COMe** and **7P-3COOEt** in solid state. (a) The thermogravimetric analysis (TGA) curves of all above compounds under nitrogen atmosphere; (b) The TGA curves of **7P-4Me** under nitrogen and air atmosphere.

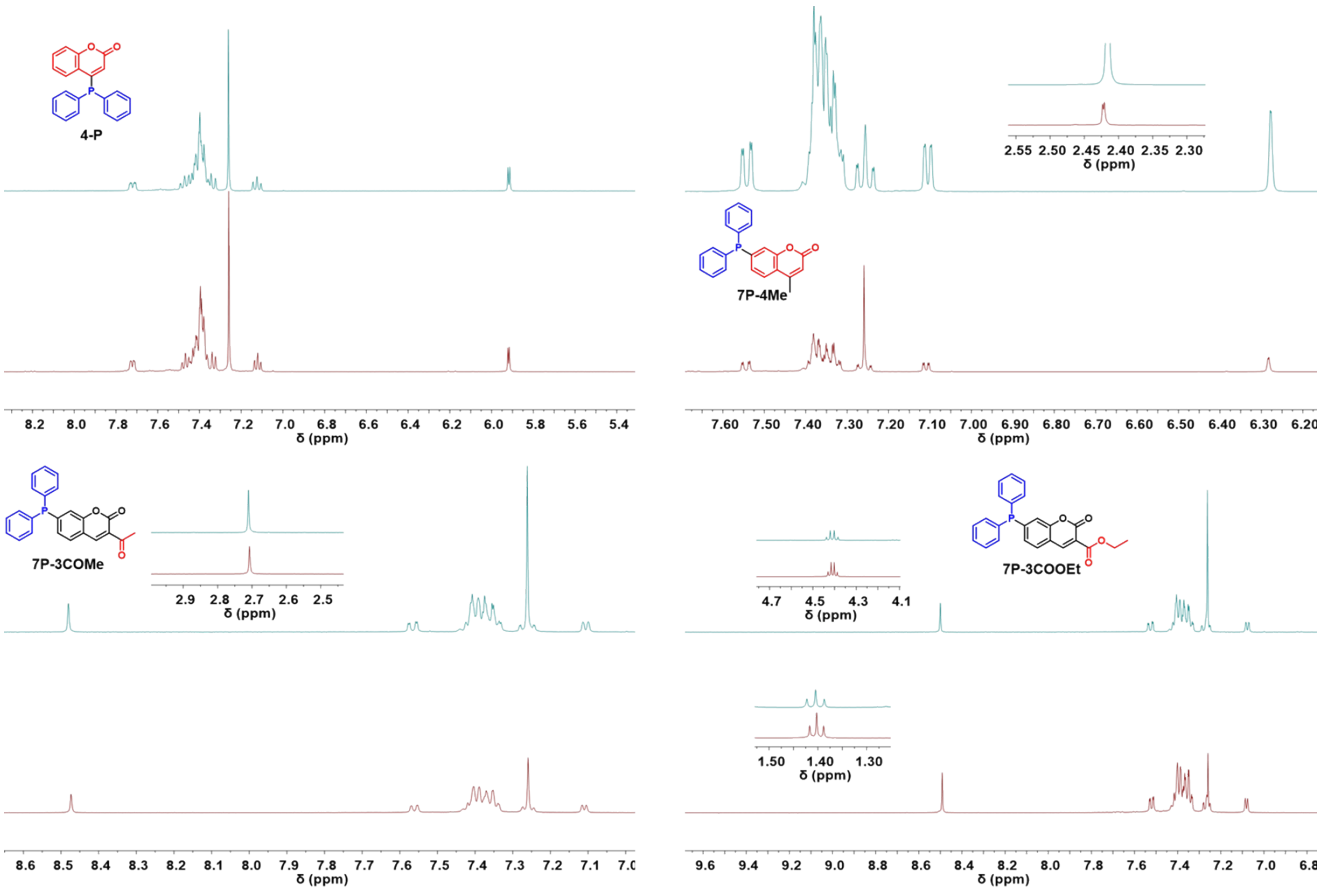

Figure S25. Photostability of **4-P**, **7P-4Me**, **7P-3COMe** and **7P-3COOEt** in solid state. The green lines represent the ^{1}H NMR data of initial compounds, and the red lines represent the ^{1}H NMR data after storage for ca. 2 years and UV light irradiation for 1.8 h (UV irradiation wavelength: 365 nm; power of UV lamp: 6 W).

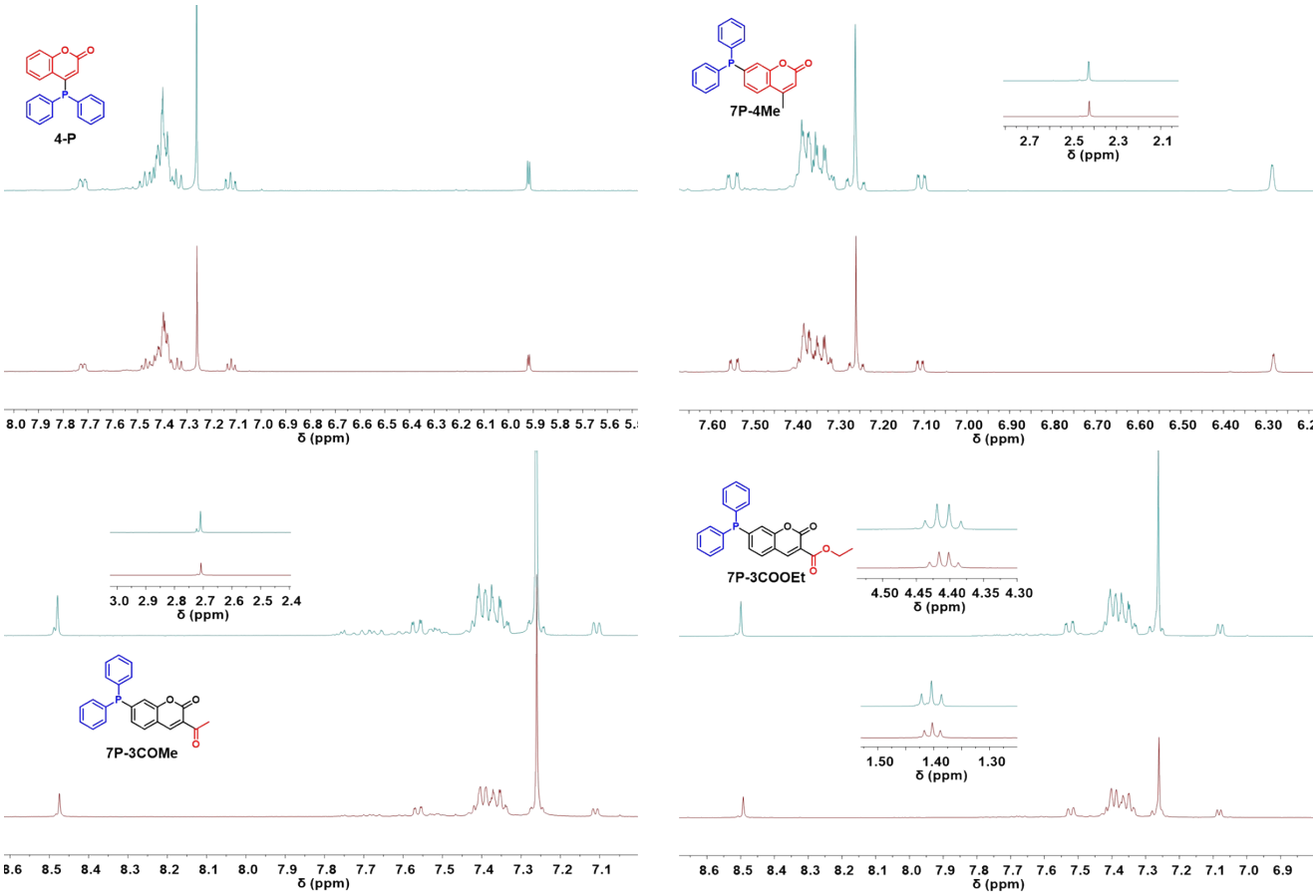

Figure S26. Photostability of **4-P**, **7P-4Me**, **7P-3COMe** and **7P-3COOEt** in solution. The green lines represent the ^{1}H NMR data of initial compounds in degassed $CDCl_3$, and the red lines represent the ^{1}H NMR data of the solution after storage for 24 h and UV light irradiation for 1 h (UV irradiation wavelength: 365 nm; power of UV lamp: 6 W).

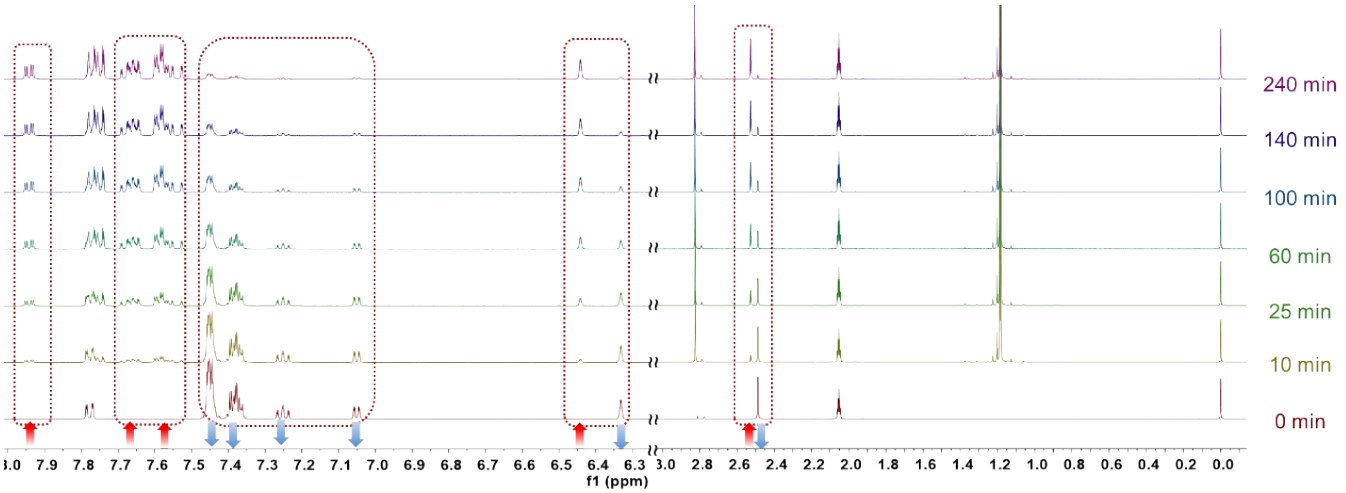

Figure S27. Oxidation process of **7P-4Me** monitored via ^{1}H NMR spectroscopy in degassed D_6-acetone containing 1.2 equiv *tert*-butyl hydroperoxide under UV light irradiation (**7P-4Me** is stable in the presence of oxidant without the external UV light irradiation. UV irradiation wavelength: 365 nm; power of UV lamp: 6 W. the corresponding oxidation product **7PO-4Me** was characterized by ^{1}H NMR and HRMS. **7PO-4Me**: ^{1}H NMR (500 MHz, D_6-acetone) δ 7.94 (dd, *J* = 8.0, 3.0 Hz, 1H), 7.76 (ddd, *J* = 11.9, 8.3, 1.4 Hz, 4H), 7.70-7.64 (m, 3H), 7.61-7.56 (m, 4H), 7.54 (dd, *J* = 12.3, 1.4 Hz, 1H), 6.44 (d, *J* = 1.4 Hz, 1H), 2.53 (d, *J* = 1.4 Hz, 3H); HRMS (ESI): m / z cal for $C_{22}H_{18}O_3P$ $[M + H]^+$: 361.0988; found: 361.0990.).

5. References

1 Y. Zhao, D. G. Truhlar, *Theor. Chem. Acc.* **2008**, *120*, 215.

2 B. P. Pritchard, D. Altarawy, B. Didier, T. D. Gibson, T. L. Windus, *Journal of chemical information and modeling* **2019**, *59*, 4814.

3 M. J. T. Frisch, G, W.; Schlegel, H. B.; Scuseria, G. E.; Robb, M. A.; Cheeseman, J. R.; Scalmani, G.; Barone, V.; Mennucci, B.; Petersson, G. A.; Nakatsuji, H.; Caricato, M.; Li, X.; Hratchian, H. P.; Izmaylov, A. F.; Bloino, J.; Zheng, G.; Sonnenberg, J. L.; Hada, M.; Ehara, M.; Toyota, K.; Fukuda, R.; Hasegawa, J.; Ishida, M.; Nakajima, T.; Honda, Y.; Kitao, O.; Nakai, H.; Vreven, T.; Montgomery, J. A., Jr.; Peralta, J. E.; Ogliaro, F.; Bearpark, M.; Heyd, J. J.; Brothers, E.; Kudin, K. N.; Staroverov, V. N.; Kobayashi, R.; Normand, J.; Raghavachari, K.; Rendell, A.; Burant, J. C.; Iyengar, S. S.; Tomasi, J.; Cossi, M.; Rega, N.; Millam, J. M.; Klene, M.; Knox, J. E.; Cross, J. B.; Bakken, V.; Adamo, C.; Jaramillo, J.; Gomperts, R.; Stratmann, R. E.; Yazyev, O.; Austin, A. J.; Cammi, R.; Pomelli, C.; Ochterski, J. W.; Martin, R. L.; Morokuma, K.; Zakrzewski, V. G.; Voth, G. A.; Salvador, P.; Dannenberg, J. J.; Dapprich, S.; Daniels, A. D.; Farkas, O.; Foresman, J. B.; Ortiz, J. V.; Cioslowski, J.; Fox, D. J. Gaussian 09, revision D.01; Gaussian, Inc.: Wallingford, CT, 2013.

4 F. Neese, *WIREs Computational Molecular Science* **2018**, *8*, e1327; B. de Souza, G. Farias, F. Neese, R. Izsák, *Journal of Chemical Theory and Computation* **2019**, *15*, 1896.

5 M. S. Hofmayer, F. H. Lutter, L. Grokenberger, J. M. Hammann, P. Knochel, *Org. Lett.* **2019**, *21*, 36.

6 M. J. Ong, R. Srinivasan, A. Romieu, J. A. Richard, *Org. Lett.* **2016**, *18*, 5122; T. Remarchuk, R. Angelaud, D. Askin, A. Kumar, A. S. Thompson, H. Cheng, J. F. Reichwein, Y. Chen, F. St-Jean, *Organic Process Research & Development* **2019**, *23*, 775.

7 N. Velusamy, A. Binoy, K. N. Bobba, D. Nedungadi, N. Mishra, S. Bhuniya, *Chem. Commun.* **2017**, *53*, 8802.

8 K. S. Kumar, M. S. Ramulu, N. P. Kumar, *New J. Chem.* **2018**, *42*, 11276.

9 B. Zhang, D. Zhan, X. Zhang, Q. Xiang, Q. Zeng, *Acta Chim. Sinica* **2012**, *70*, 1655.

6. NMR Spectra of Synthesized Compounds

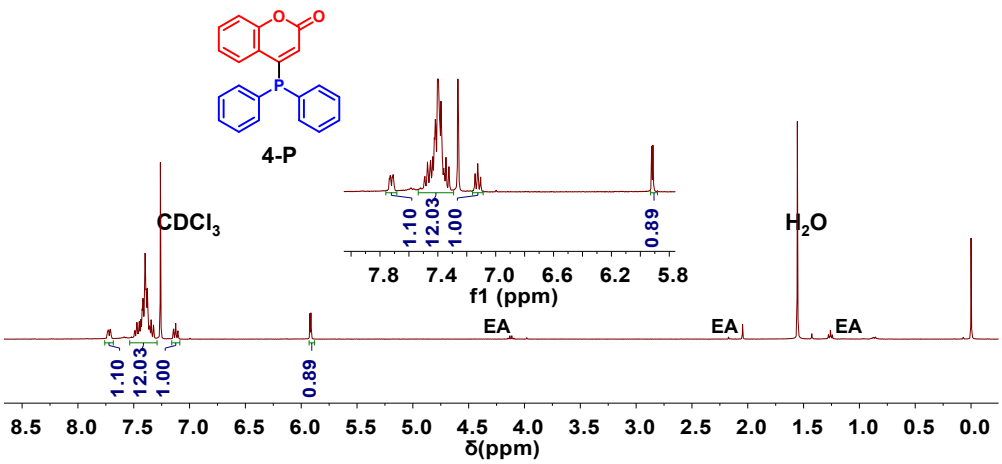

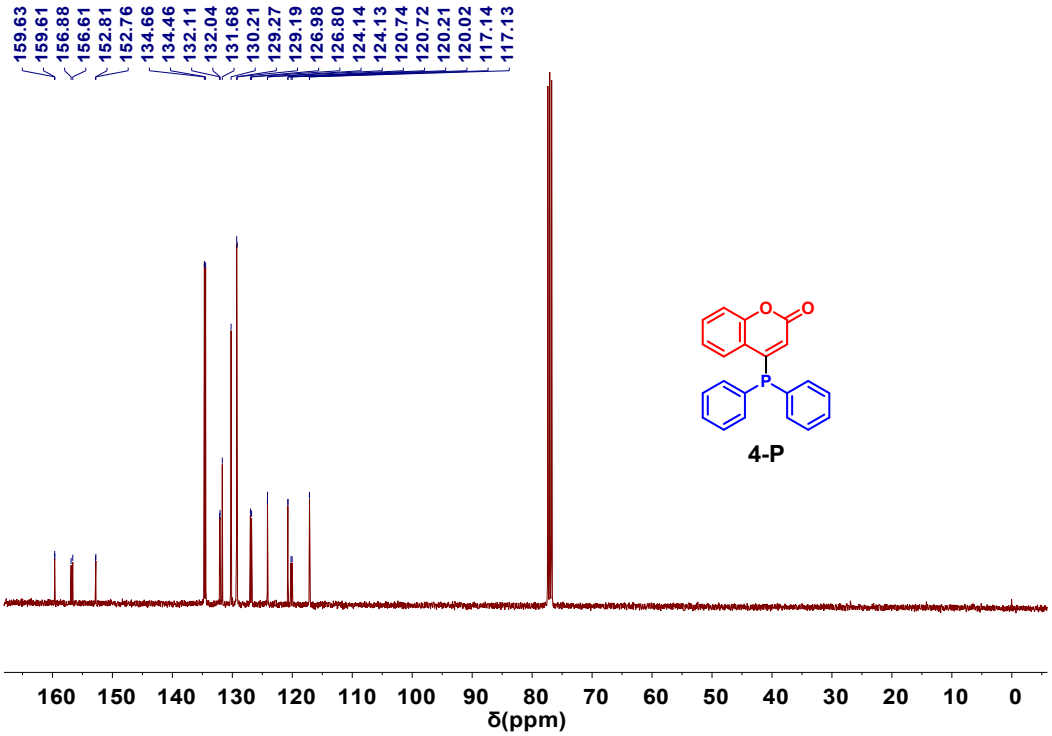


7.55
7.55
7.53
7.53
7.40
7.39
7.39
7.38
7.38
7.37
7.37
7.36
7.36
7.35
7.35
7.34
7.33
7.33
7.32
7.32
7.31
7.31
7.28
7.27
7.26
7.26
7.24
7.24
7.11
7.11
7.10
7.10
6.28
2.42
2.41

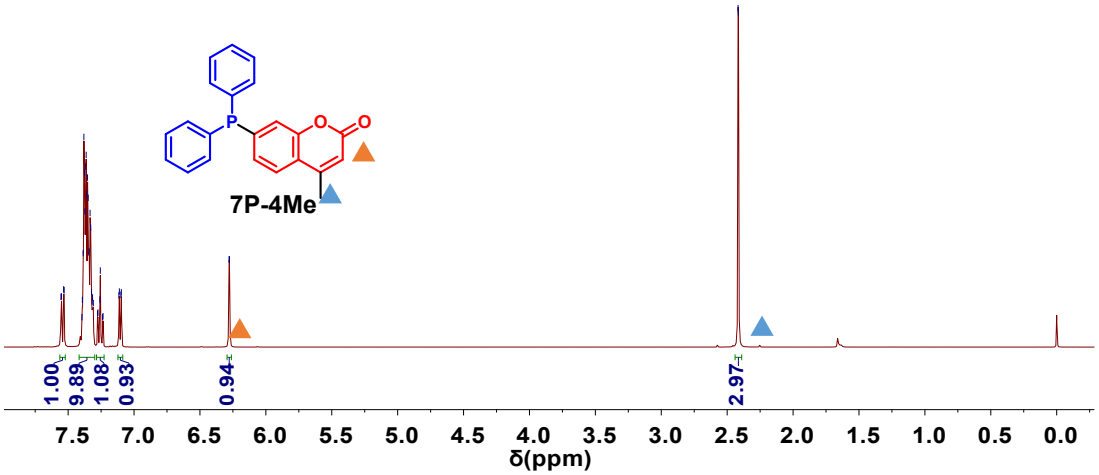
7P-4Me
1.00
9.89
1.08
0.93
0.94
2.97
7.5
7.0
6.5
6.0
5.5
5.0
4.5
4.0
3.5
3.0
2.5
2.0
1.5
1.0
0.5
0.0
δ(ppm)

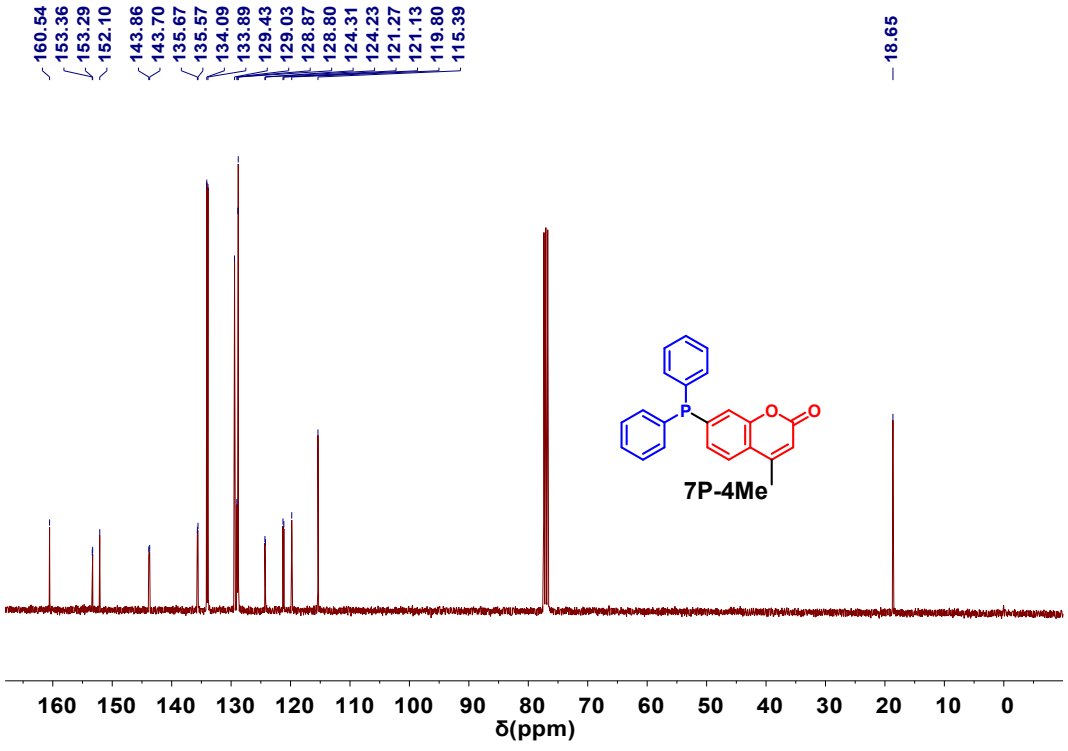
160.54
153.36
153.29
152.10
143.86
143.70
135.67
135.57
134.09
133.89
129.43
129.03
128.87
128.80
124.31
124.23
121.27
121.13
119.80
115.39
18.65
7P-4Me
160
150
140
130
120
110
100
90
80
70
60
50
40
30
20
10
0
δ(ppm)

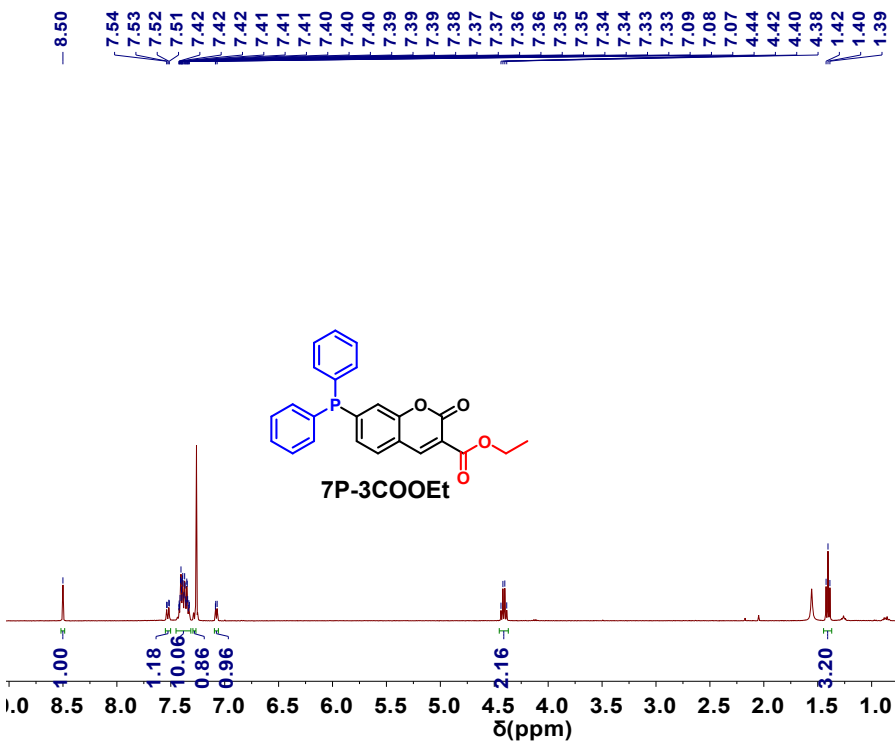
8.50
7.54
7.53
7.52
7.51
7.42
7.42
7.42
7.41
7.41
7.41
7.40
7.40
7.40
7.39
7.39
7.39
7.38
7.37
7.37
7.36
7.36
7.35
7.35
7.34
7.34
7.33
7.33
7.09
7.08
7.07
4.44
4.42
4.40
4.38
1.42
1.40
1.39
7P-3COOEt
1.00
1.18
10.06
0.86
0.96
2.16
3.20
δ(ppm)

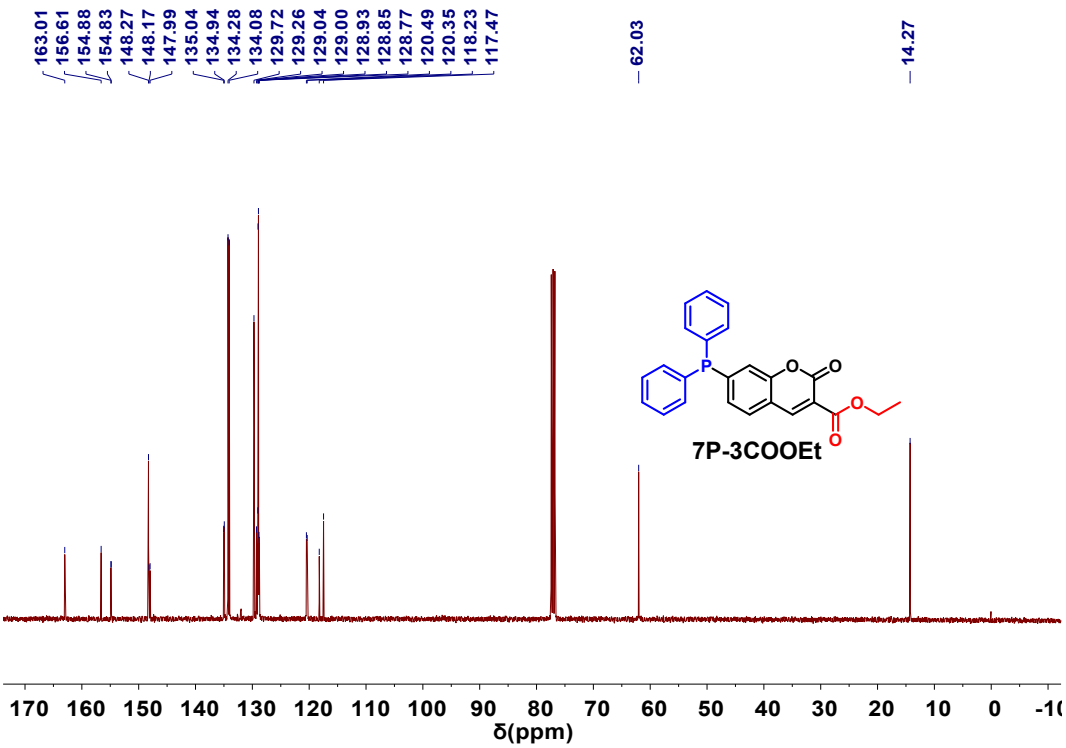
163.01
156.61
154.88
154.83
148.27
148.17
147.99
135.04
134.94
134.28
134.08
129.72
129.26
129.04
129.00
128.93
128.85
128.77
120.49
120.35
118.23
117.47
62.03
14.27
7P-3COOEt
δ(ppm)

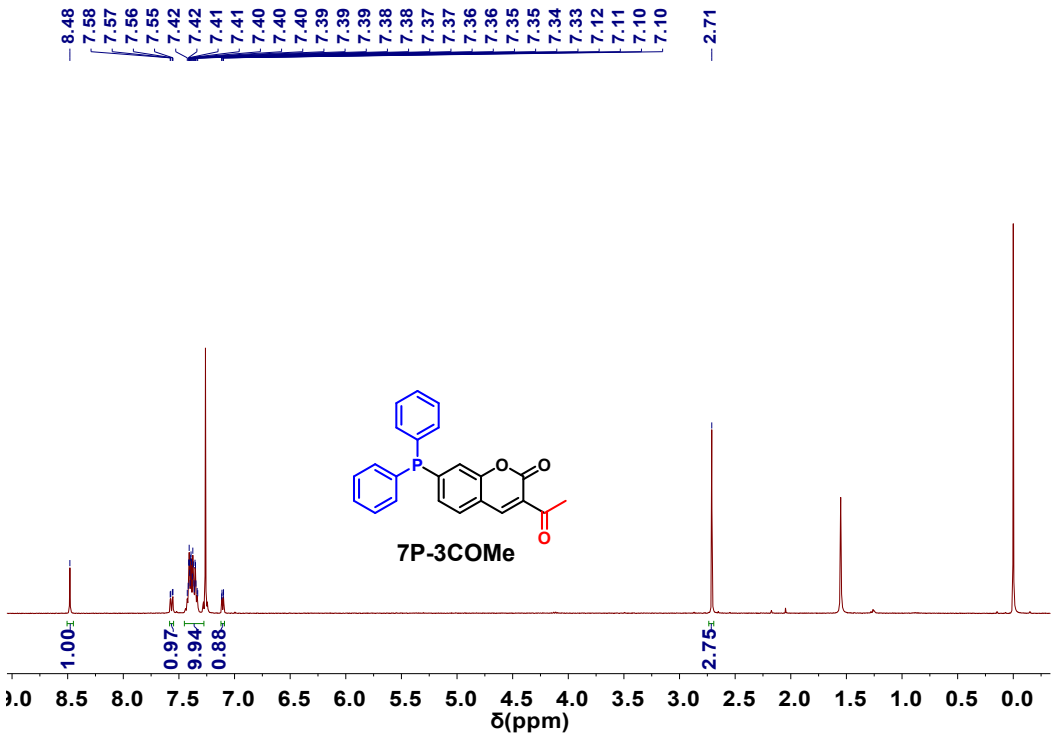
8.48
7.58
7.57
7.56
7.55
7.42
7.42
7.41
7.41
7.40
7.40
7.40
7.39
7.39
7.39
7.38
7.38
7.37
7.37
7.36
7.36
7.35
7.35
7.34
7.33
7.12
7.11
7.10
7.10
2.71
7P-3COMe
1.00
0.97
9.94
0.88
2.75
δ(ppm)

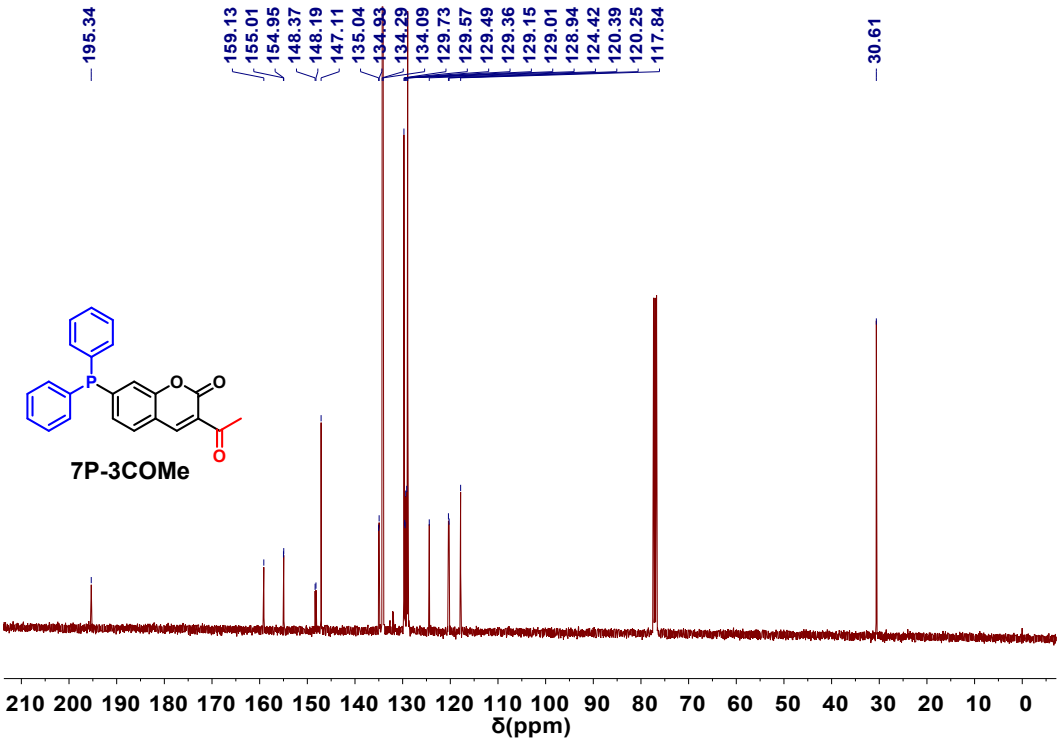
195.34
159.13
155.01
154.95
148.37
148.19
147.11
135.04
134.93
134.29
134.09
129.73
129.57
129.49
129.36
129.15
129.01
128.94
124.42
120.39
120.25
117.84
30.61
7P-3COMe
δ(ppm)

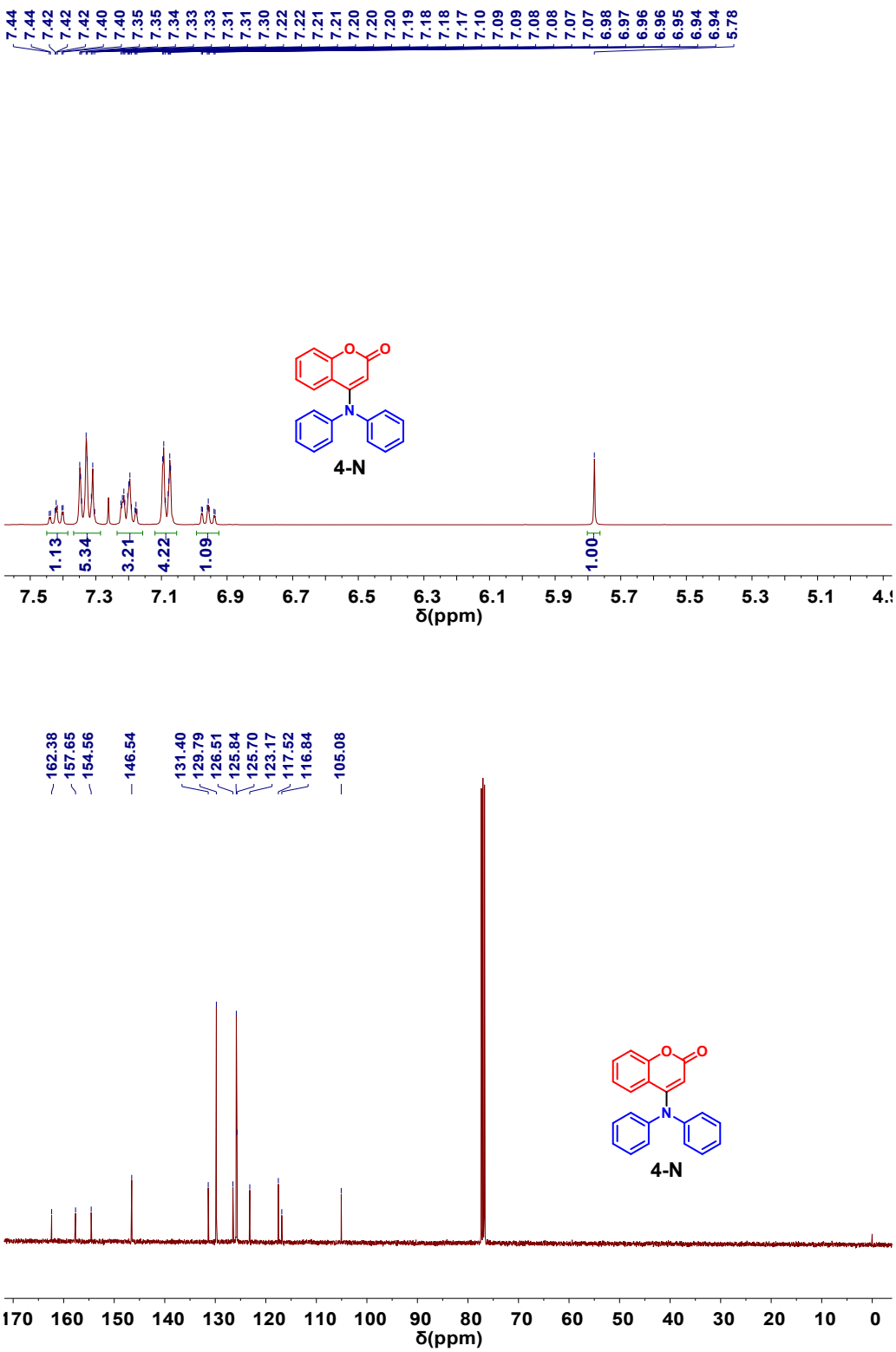
7.44 7.44 7.42 7.42 7.42 7.40 7.40 7.35 7.35 7.34 7.33 7.33 7.31 7.31 7.30 7.22 7.21 7.21 7.20 7.20 7.19 7.18 7.18 7.17 7.10 7.09 7.09 7.08 7.08 7.07 7.07 6.98 6.97 6.96 6.96 6.95 6.94 6.94 5.78
4-N
1.13 5.34 3.21 4.22 1.09 1.00
7.5 7.3 7.1 6.9 6.7 6.5 6.3 6.1 5.9 5.7 5.5 5.3 5.1
δ(ppm)
162.38 157.65 154.56 146.54 131.40 129.79 126.51 125.84 125.70 123.17 117.52 116.84 105.08
4-N
170 160 150 140 130 120 110 100 90 80 70 60 50 40 30 20 10 0
δ(ppm)

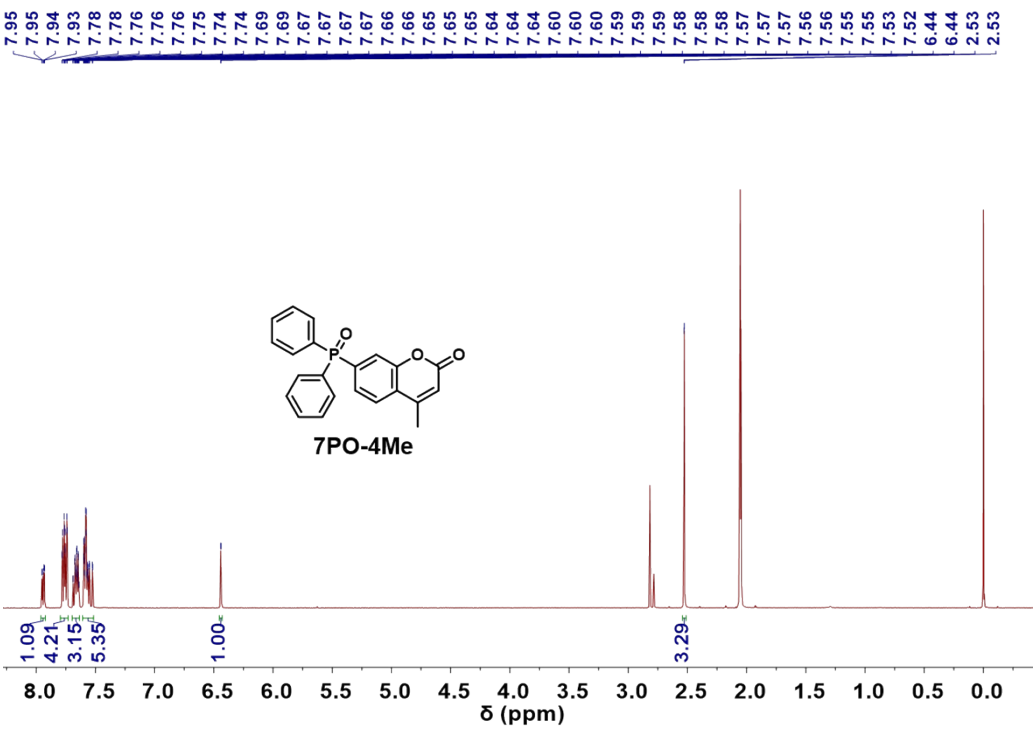
7PO-4Me
1.09
4.21
3.15
5.35
1.00
3.29
δ (ppm)